Deuteron Photodisintegration at Intermediate Energies*

J. M. BERGER†
Case Institute of Technology, Cleveland, Ohio
(Received February 9, 1954)

The differential and total cross sections for the photodisintegration of the deuteron are calculated for incident gamma-ray energies in the range from 6 to 28 Mev. The following cases are treated: (1) Approximation I, in which shape-independent wave functions are used corresponding to a 50 percent charge-exchange central force, (2) Approximation II-C, in which a central Hulthén potential with a variable percentage of charge exchange forces is used, (3) Approximation II-NC, in which approximate noncentral Hulthén wave functions and an approximate noncentral Hulthén potential with 50 percent charge-exchange force, is used. In all these calculations, use is made (where possible) of a form for the interaction between the deuteron and radiation that gives the results of the interaction to all multipole orders automatically. We also estimate the possible effect of exchange currents on the cross sections by a calculation making use of the phenomenologically derived exchange moments of Berger and Foldy.

The numerical results of these calculations are used to estimate the uncertainty in the theoretically calculated cross section at the present time. It is concluded that the uncertainty may be as large as 15 percent of the total cross section for these energies. About 5 percent of this arises from experimental uncertainties in empirically determined parameters, while the remainder arises from ignorance of the exact form of the neutron-proton interaction.

I. INTRODUCTION

THE problem of the experimental determination of absolute cross sections for photoprocesses in nuclei is complicated by the lack of a reliable method of fixing the spectrum of the incident gamma rays employed in the experiment. One promising method of obtaining a good absolute cross-section measurement is to use as a standard for calibration the simultaneously observed deuteron photodisintegration which may then be compared to the theoretical prediction for this process.[1] Unfortunately, although the deuteron is the simplest nuclear system of interest, it is far from being completely understood, and, as a result, there remain various sources of uncertainty in the theoretically predicted cross section. We wish, in this paper, to undertake a comprehensive and systematic calculation of the deuteron photodisintegration cross section. The results of such a calculation are, of course, of interest in themselves, but we hope that they will also serve to better evaluate the accuracy of our present knowledge of this problem and thereby to indicate the reliability of the above scheme as a calibration method.

We will restrict ourselves to the consideration of incident photon energies in the range from about 6 Mev to 30 Mev although, as will be indicated later, the methods used are applicable to lower and to higher energies and are perhaps even more valuable in the latter region. Our reasons for this choice of energy range are twofold: firstly, much of the investigation of photoprocesses is taking place in this energy region, and secondly, the Case betatron, which has been engaged in investigating such processes, is limited to energies of the order of 30 Mev. A further impetus to a careful analysis in this energy range is the growing accurcy of measurements of the total and differential cross sections for the photodisintegration of the deuteron at these energies.[2,3]

An accurate theoretical prediction of the photodisintegration cross section depends, of course, on knowledge of the correct form of the interaction of the deuteron with the electromagnetic field and further on knowledge of the initial and final wave functions for the deuteron system. Our knowledge of both these aspects of the problem is insufficient to allow an exact calculation to be made and it is therefore necessary to employe approximations, using with discretion what information is available. We are favored in this approach by several circumstances: We are cognizant of what are probably the most important terms in the interaction of the deuteron with radiation and we can at least estimate the effects of those terms of which our knowledge is more scanty. Furthermore, while detailed knowledge of the interaction potential between proton and neutron is necessary for an exact calculation of initial and final wave functions for the deuteron photodisintegration, yet many of the most important features of these wave functions, insofar as they determine the transition matrix element, can be derived on a semiempirical basis. Hence those features of the wave functions which depend on details of the potential interaction introduce considerably smaller uncertainties into the results than might otherwise be the case.

Before describing in detail the nature of our approach and approximations to this problem, we shall summarize briefly some of the more recent calculations of the deuteron photodisintegration cross section by Bethe

* From a thesis submitted to Case Institute of Technology in partial fulfillment of the requirements for the degree of Doctor of Philosophy.

† U. S. Atomic Energy Commission Pre-doctoral fellow, now at Forrestal Research Center, Princeton University, Princeton, New Jersey.

[1] V. E. Krohn, Jr., and E. F. Shrader, Phys. Rev. 87, 685 (1952).

[2] Barnes, Carver, Stafford, and Wilkinson, Phys. Rev. 86, 359 (1952).

[3] V. E. Krohn, Jr., and E. F. Shrader, Phys. Rev. 86, 391 (1952).

and Longmire,[4] Schiff,[5] Marshall and Guth,[6] and Feshbach and Schwinger[7] in order to illuminate the distinguishing features of these and our own calculations.

Bethe and Longmire are concerned in their paper with energies less than 10 Mev and therefore they are able to express their results in a form largely independent of the specific internucleonic potential. They exhibit the electric and magnetic dipole matrix elements in terms of the triplet and singlet effective ranges, assuming a central force character for the internucleonic potential and the absence of interaction in odd parity states of the system (that is, they assume a Serber potential of half ordinary and half charge-exchange character). The results for the magnetic dipole term are checked by explicit calculations using different well shapes: square, Hulthén, and exponential. They also indicate that the electric dipole cross section is slightly smaller at these energies if 100 percent charge exchange forces are assumed in place of Serber forces.

Schiff calculates for the energy region of 20 to 140 Mev only the photoelectric effect, omitting the photomagnetic effect because of the uncertainty due to exchange currents. On the assumption of central forces of half charge-exchange, half ordinary, character, he examines the long-tailed potentials, exponential and Yukawa, and calculates in the electric dipole and quadrupole approximations. It is shown that the quadrupole term interferes with the dipole term so that the quadrupole term has an appreciable effect on the angular distribution. It is also shown that there is little difference between the cross sections obtained with the differently shaped wells, especially below 50 Mev.

Marshall and Guth have performed a similar calculation to that of Schiff, including the magnetic quadrupole term, obtaining essentially the same results. They also calculate the photodisintegration cross section for a square well with different percentages of charge exchange. The results they find for the square well with 50 percent charge exchange are quite different from those with the long-tailed potentials at high energies but are closely the same for energies below 30 Mev. The effect of large variations of the percentage of charge exchange they find to have a large effect at all energies.[8]

Feshbach and Schwinger have calculated the photodisintegration cross section for energies up to 20 Mev with noncentral forces having 50 percent charge-exchange character in the electric and magnetic dipole approximations. They find the electric dipole term to be essentially the shape-independent term of Bethe and Longmire. In the magnetic dipole calculation they include a term corresponding to the exchange current contribution, and by comparison with experiment, conclude that this contribution is small.

In our treatment of the photodisintegration problem we shall consider all of the effects mentioned above although in varying degree. Our calculation is based on an assumed form for the interaction between the deuteron and the electromagnetic field which is derived in an earlier paper.[9] (In the initial calculations only the so-called "one-particle" terms are considered.) This formulation of the interaction has the advantage that it allows us to include automatically and in one step all of the multipole orders in which the photodisintegration process takes place with relatively little extra labor. Estimates of the contributions of what are called in reference 9 "interaction terms" are made in the later calculations of the magnetic dipole matrix element by making use of results obtained from the phenomenological treatment of exchange moments by Berger and Foldy,[10] in the absence of exact expressions that would be predicted by a correct meson theory.

Once the form of the deuteron-radiation interaction has been assumed, the calculation of the matrix elements requires knowledge of the appropriate initial- and final-state wave functions for the deuteron. These are handled in our calculations in the following way: We assume, in what we shall call Approximation I, wave functions for the initial and final state which can be specified without any direct reference to the exact form of the interaction potential between neutron and proton. We do this as follows: For the initial wave function, representing the ground state of the deuteron, we follow Bethe and Longmire in employing a wave function appropriate to a zero-range interaction between neutron and proton but with a normalization adjusted by the employment of the empirical effective range of the neutron-proton interaction to corespond to that of a potential interaction of the proper effective range. This wave function can then be completely expressed once we are given the empirical triplet effective range and the deuteron binding energy. The final-state wave function, in this approximation, is assumed to be a plane wave as if the neutron and proton were free, but with one modification. The S-wave part of the plane wave is modified by the introduction of an empirical phase shift for both the singlet and triplet spin states so as to take partial account of the neutron-proton interaction. The final-state wave functions may therefore also be thought of as arising from a potential of zero range. The phase shifts employed are those deriving from the empirically known values of the zero energy scattering lengths and effective ranges of the singlet and triplet deuteron interactions, neglecting the contribution of "shape-dependent" terms. Thus the

[4] H. A. Bethe and C. Longmire, Phys. Rev. **77**, 647 (1950).
[5] L. I. Schiff, Phys. Rev. **78**, 733 (1950).
[6] J. F. Marshall and E. Guth, Phys. Rev. **78**, 738 (1950).
[7] H. Feshbach and J. Schwinger, Phys. Rev. **84**, 194 (1951).
[8] This result is in disagreement with our own results. It is believed to arise from several minor but numerically significant errors in the formulas of Marshall and Guth. See reference 14 of the present paper.
[9] L. L. Foldy, Phys. Rev. **92**, 178 (1953).
[10] J. M. Berger and L. L. Foldy, Tech. Report No. 18 at the Nuclear Physics Laboratory of Case Institute of Technology. These results will be published in a modified form.

final-state wave functions in this approximation can also be completely written down once these empirical parameters are given. We may also note that insofar as final states of odd parity are concerned, these assumed forms for the final-state wave functions correspond exactly to a Serber potential with 50 percent exchange force. The calculations in this Approximation I correspond then very closely to those of Bethe and Longmire but may be utilized over a higher energy range as a result of including automatically all multipoles in the calculation. This calculation, Approximation I, serves as a basis with which we may compare the changes that result from the more detailed calculations.

The second approximation in our calculation distinguishes between two cases corresponding to central and to noncentral forces between neutron and proton. In the first of these which we call Approximation II-C, we calculate the modification in the matrix elements and in the calculated cross sections resulting from the changes in the initial- and final-state wave functions when a specific radial dependence is assumed for a central interaction between the neutron and proton and when the percentage of charge-exchange character of this interaction is varied. The calculation is made with the choice of the Hulthén potential for the radial dependence of the interaction potential. The effects of modifications in the initial- and final-state wave functions are separately calculated. Where convenient and appropriate some additional approximations are made in these calculations. The contributions of exchange moment terms in the deuteron-radiation interaction are considered separately.

The second form of the second approximation, which is called Approximation II-NC, is similar to Approximation II-C, but the effects of a noncentral (tensor) character of the potential interaction between neutron and proton are examined instead.

In Sec. II the form of the interaction used is described together with the appropriate symbols. In Sec. III the details of the calculations are given excepting those for the exchange moments, and in Sec. IV the results are described. The details of the exchange moment contribution calculation are discussed in Sec. V. In Sec. VI we discuss the over-all results of this paper.

II. INTERACTION

To represent the interaction of radiation with the deuteron we will use the form of the general equations appropriate to the deuteron for the nuclear photoeffect derived by Foldy.[9] This form of the interaction will then give us the effects of all multipoles while involving very little more work for most of the calculations than is usually entailed in obtaining the matrix elements in the dipole approximation of the usual multipole expansion. Its only disadvantage is the somewhat more cumbersome form of the resultant matrix elements, although it is usually quite simple to reduce them to the corresponding dipole terms for comparison.

Our form of the interaction operator

$$\mathcal{H}' = -\int \mathbf{j}\cdot\mathbf{A}\,d\tau,$$

is conveniently expressed as the sum of four terms.

$$\mathcal{H}' = \mathcal{E} + \mathfrak{M}_c + \mathfrak{M}_s + \mathfrak{M}_x. \tag{1}$$

We label these terms in the following fashion. $\mathcal{E}$ is termed the electric interaction, $\mathfrak{M}_c$ is termed the magnetic convection interaction, $\mathfrak{M}_s$ is the magnetic spin interaction, and $\mathfrak{M}_x$ is the magnetic exchange interaction. In the next two sections we will confine our attention to the first three interactions: however, in Sec. V we will treat some aspects of the magnetic exchange interaction, although in only the dipole approximation.

Then the forms of the matrix elements corresponding to the interaction of a photon of wave vector $\boldsymbol{\kappa}$ with the deuteron in the center-of-mass (zero-momentum) system may be written as[9]

$$\begin{aligned}
E &= (\Psi_f|\mathcal{E}|\Psi_g) = \left(\frac{2\pi\hbar c}{\kappa V}\right)^{\frac{1}{2}} \frac{ie}{2\hbar c}(\epsilon_f - \epsilon_0) \\
&\quad \times \left(\Psi_f \left| \int_0^1 \boldsymbol{\varepsilon}\cdot\mathbf{r} \exp(i\boldsymbol{\kappa}\cdot\mathbf{R})[\tau_1{}^P \exp(is\boldsymbol{\kappa}\cdot\mathbf{r}/2) \right.\right. \\
&\qquad \left.\left. - \tau_2{}^P \exp(-is\boldsymbol{\kappa}\cdot\mathbf{r}/2)]ds \right| \Psi_g \right), \\
M_c &= (\Psi_f|\mathfrak{M}_c|\Psi_g) = \left(\frac{2\pi\hbar c}{\kappa V}\right)^{\frac{1}{2}} \frac{ie}{2\hbar c}(\epsilon_f - \epsilon_0) \\
&\quad \times \left(\Psi_f \left| \frac{\hbar\kappa c}{\epsilon_0 - \epsilon_f}\cdot\frac{1}{Mc}\int_0^1 \{\tau_1{}^P([\mathbf{r}\times\mathbf{p}]\right.\right. \\
&\qquad \cdot\boldsymbol{\varepsilon}' \exp(is\boldsymbol{\kappa}\cdot\mathbf{r}/2) + \exp(is\boldsymbol{\kappa}\cdot\mathbf{r}/2)\boldsymbol{\varepsilon}'\cdot[\mathbf{r}\times\mathbf{p}]) \\
&\qquad + \tau_2{}^P([\mathbf{r}\times\mathbf{p}]\cdot\boldsymbol{\varepsilon}' \exp(-is\boldsymbol{\kappa}\cdot\mathbf{r}/2) \\
&\qquad \left.\left. + \exp(-is\boldsymbol{\kappa}\cdot\mathbf{r}/2)\boldsymbol{\varepsilon}'\cdot[\mathbf{r}\times\mathbf{p}])\} \exp(i\boldsymbol{\kappa}\cdot\mathbf{R})sds, \right| \Psi_g \right), \\
M_s &= (\Psi_f|\mathfrak{M}_s|\Psi_g) = \left(\frac{2\pi\hbar c}{\kappa V}\right)^{\frac{1}{2}} \frac{ie}{2\hbar c}(\epsilon_f - \epsilon_0) \\
&\quad \times \left(\Psi_f \left| \frac{\hbar\kappa c}{(\epsilon_0 - \epsilon_f)}\frac{\hbar}{Mc} \exp(i\boldsymbol{\kappa}\cdot\mathbf{R}) \right.\right. \\
&\qquad \times \{(\mu_P\tau_1{}^P + \mu_n\tau_1{}^n)\boldsymbol{\sigma}_1\cdot\boldsymbol{\varepsilon}' \exp(i\boldsymbol{\kappa}\cdot\mathbf{r}/2) \\
&\qquad \left.\left. + (\mu_P\tau_2{}^P + \mu_n\tau_2{}^n)\boldsymbol{\sigma}_2\cdot\boldsymbol{\varepsilon}' \exp(-i\boldsymbol{\kappa}\cdot\mathbf{r}/2)\} \right| \Psi_g \right),
\end{aligned} \tag{2}$$

where Ψ_f and Ψ_g are the final- and ground-state wave functions, respectively.

In the above equations it will be noted that the multiplying factors outside the brackets have been written the same in all three cases, i.e., $(2\pi\hbar c/\kappa V)^{\frac{1}{2}}(ie/2\hbar c)(\epsilon_f-\epsilon_0)$, so that the quantities inside the brackets serve to indicate the relative magnitudes of these matrix elements. For the energies of interest in this paper the distinction between $\hbar\kappa c$, the photon energy, and $(\epsilon_f-\epsilon_0)$, the change in the internal energy of the deuteron, is negligible. Hence, for example, the magnitude of M_c relative to E is of order p/Mc, where p is the relative particle momentum.

The symbols used in the above expressions for the matrix elements represent the following: V is the normalization volume of the incident photon, $(\epsilon_f-\epsilon_0)$ is the difference between the internal energy states of the deuteron before and after the absorption of the photon, $\mathbf{R}$ is the center-of-mass coordinate, $\mathbf{r}$ is the relative coordinate of the neutron and proton, $\mathbf{p}$ is the momentum conjugate to $\mathbf{r}$, $\boldsymbol{\varepsilon}$ is the electric polarization vector of the incident photon, $\boldsymbol{\varepsilon}'=[\boldsymbol{\kappa}\times\boldsymbol{\varepsilon}]/\kappa$ is the magnetic polarization vector of the incident photon, M is the proton mass and is taken equal to the neutron mass, μ_P is the magnetic moment of the proton expressed in number of nuclear magnetons, μ_n is the magnetic moment of the neutron expressed in number of nuclear magnetons, $\boldsymbol{\sigma}_i$ is the spin operator associated with the ith nucleon, τ_i^P is the proton projection operator for the ith nucleon with $\tau_i^P=(1+\tau_i^z)/2$, τ_i^n is the neutron projection operator for the ith nucleon with $\tau_i^n=(1-\tau_i^z)/2$, τ_i^z is the z component of the isotopic spin operator, and s is a parameter of integration.

In the calculations that follow it will be convenient to separate the magnetic spin matrix element M_s into two terms, M_{st} corresponding to transitions due to the magnetic spin interaction $\mathfrak{M}_s$ to final triplet spin states, and M_{ss} corresponding to transitions to final singlet spin states.

III. CALCULATIONS

The wave functions that will be used in the calculation of the matrix elements described in the previous section, Eqs. (2), will be given here. The general form of the wave functions will be written in the following manner:

$$\Psi_g=\psi_g^0+\psi_g^1, \quad \Psi_f=\psi_f^0+\psi_f^1, \tag{3}$$

where ψ_g^0 is the shape-independent ground-state wave function and ψ_g^1 represents the correction to the shape-independent ground-state wave function due to the choice of a shape-dependent potential, in our case, a Hulthén potential. Similarly ψ_f^0 is the shape-independent final-state wave function corresponding to a plane wave except for a modified S state in which a phase shift is introduced to account for interaction, and ψ_f^1 is the correction introduced because of our specific choice of potential. It is more convenient to indicate the spin multiplicity of the final states explicitly. Thus, Ψ_{ft} is the triplet final-state wave function that is used in the calculation of the E, M_c, and M_{st} matrix elements, and Ψ_{fs} is the singlet final-state wave function that is used in the calculation of the M_{ss} matrix elements.

Thus the matrix elements described in II may be written as the sum of terms, in such a fashion that the introduction of each correction gives rise to an individual term so that the effects of each correction may be easily observed. Thus, for example, we may write E as

$$E=(\Psi_{ft}|\mathcal{E}|\Psi_g)={}_0E^0+{}_0E^1+{}_1E^0+{}_1E^1, \tag{4}$$

where

$$\begin{aligned} {}_0E^0&=(\psi_{ft}^0|\mathcal{E}|\psi_g^0), \quad {}_0E^1=(\psi_{ft}^0|\mathcal{E}|\psi_g^1),\\ {}_1E^0&=(\psi_{ft}^1|\mathcal{E}|\psi_g^0), \quad {}_1E^1=(\psi_{ft}^1|\mathcal{E}|\psi_g^1). \end{aligned} \tag{5}$$

We will speak of the calculation as being done in two approximations, Approximation I and Approximation II. In Approximation I only shape-independent effects are considered and thus it consists of the calculations of the ${}_0E^0$, ${}_0M_c^0$, ${}_0M_{st}^0$, ${}_0M_{ss}^0$ matrix elements. These terms will serve as a reference to which we may compare the effects calculated in the Approximation II. In the second Approximation the modifications that are introduced by the consideration of such effects as the explicitly Hulthén well shape, central and noncentral forces, and interactions in the final states, are calculated. These effects are introduced by the choice of the wave function corrections ψ_g^1, ψ_f^1. In this approximation the matrix elements we will actually calculate are ${}_0E^1$, ${}_1E^0$, ${}_0M_{ss}^1$, ${}_1M_{ss}^0$, ${}_1M_{ss}^1$. The details of these two approximations follow.

A. Approximation I

In this approximation we will calculate four matrix elements corresponding to the four interactions $\mathcal{E}$, $\mathfrak{M}_c$, $\mathfrak{M}_{st}$, $\mathfrak{M}_{ss}$ described in Sec. II, making use of only shape-independent wave functions. The $\mathfrak{M}_{st}$ and $\mathfrak{M}_{ss}$ interactions are, of course, exactly the same, both being the $\mathfrak{M}_s$ described in II. This notation is however convenient in denoting explicitly the spin multiplicity of the final-state wave function that is used with the $\mathfrak{M}_s$ interaction to obtain the matrix element M_{st} or M_{ss}. The wave functions we will use in this calculation are ψ_g^0 for the ground-state function and ψ_{ft}^0 or ψ_{fs}^0 for the final-state function, where ψ_{fs}^0 is used only with $\mathfrak{M}_{ss}$. For ψ_g^0 we will take the zero range form for the deuteron ground state, in which the correction for the finite range of forces is taken into account in the usual manner through the use of the effective range.[11] Thus

$$\psi_g^0=V^{-\frac{1}{2}}\exp(-i\boldsymbol{\kappa}\cdot\mathbf{R})\left[\frac{2\alpha}{4\pi(1-\alpha r_{0t})}\right]^{\frac{1}{2}}\frac{e^{-\alpha r}}{r}\cdot 2^{-\frac{1}{2}}(\xi_1\eta_2-\xi_2\eta_1)\chi_g^t. \tag{6}$$

For the final-state wave functions $\psi_{fs,t}^0$ we will use a plane wave except for replacing the S part by an S

[11] H. A. Bethe, Phys. Rev. 76, 38 (1949).

wave function in which the interaction in the final S state has been considered by the use of the phase shift δ_0. Therefore, we have for the triplet final-state wave function:

$$\psi_{ft}{}^0=V^{-1}2^{-\frac{1}{2}}\Big\{\xi_1\eta_2e^{i\mathbf{k}\cdot\mathbf{r}}-\xi_2\eta_1e^{-i\mathbf{k}\cdot\mathbf{r}}-[\xi_1\eta_2-\xi_2\eta_1]\times\Big[\frac{\sin kr}{kr}-e^{-i\delta_{0t}}\frac{\sin(kr+\delta_{0t})}{kr}\Big]\Big\}\chi_f{}^t, \quad (7)$$

and for the singlet final-state function:

$$\psi_{fs}{}^0=V^{-1}2^{-\frac{1}{2}}\Big\{\xi_1\eta_2e^{i\mathbf{k}\cdot\mathbf{r}}+\xi_2\eta_1e^{-i\mathbf{k}\cdot\mathbf{r}}-[\xi_1\eta_2+\xi_2\eta_1]\times\Big[\frac{\sin kr}{kr}-e^{-i\delta_{0s}}\frac{\sin(kr+\delta_{0s})}{kr}\Big]\Big\}\chi_f{}^s. \quad (8)$$

In the above, the symbols used mean the following: $\mathbf{k}$ is the propagation vector of the proton and k its magnitude, ξ_i and η_i are isotopic spin wave functions with ξ_i corresponding to the ith particle being in a proton state while η_i corresponds to the ith particle in a neutron state. The χ's are spin wave functions, with $\chi_g{}^t$ the ground-state triplet spin, while $\chi_f{}^t$ and $\chi_f{}^s$ are, respectively, the final-state triplet and singlet spin wave functions. Finally, r_{0t} is the triplet effective range, and δ_{0t} and δ_{0s} are, respectively, the phase shifts of the final-state triplet and singlet S wave functions obtained from the usual formula[11,12]

$$k\cot\delta_0=-a^{-1}+\tfrac{1}{2}k^2r_0,$$

where a is the appropriate scattering length and r_0 the appropriate effective range.

The values of the constants we use are, with the exception of r_{0t}, the same as used by Bethe and Longmire, and are

$$\alpha=2.31\times10^{12}\text{ cm}^{-1},\quad a_t=0.528\times10^{-12}\text{ cm},$$
$$a_s=-2.375\times10^{-12}\text{ cm},$$
$$r_{0t}=1.70\times10^{-13}\text{ cm},\quad r_{0s}=2.4\times10^{-13}\text{ cm},$$

corresponding to a binding energy for the deuteron of 2.235 Mev.

The wave functions just described will now be used to evaluate the matrix elements ${}_0E^0$, ${}_0M_c{}^0$, ${}_0M_{st}{}^0$, ${}_0M_{ss}{}^0$ where

$$\begin{aligned}{}_0E^0&=(\psi_{ft}{}^0|\,\mathcal{E}\,|\psi_g{}^0),\qquad {}_0M_c{}^0=(\psi_{ft}{}^0|\,\mathfrak{M}\,|\psi_g{}^0),\\ {}_0M_{st}{}^0&=(\psi_{ft}{}^0|\,\mathfrak{M}\,|\psi_g{}^0),\quad {}_0M_{ss}{}^0=(\psi_{fs}{}^0|\,\mathfrak{M}\,|\psi_g{}^0).\end{aligned} \quad (9)$$

The resulting matrix elements after integration but before the summation and averaging over the spin states and polarizations have been performed are

$${}_0E^0=\Big(\frac{2\pi\hbar c}{\kappa V^2}\cdot\frac{2\pi\alpha}{1-\alpha r_{0t}}\Big)^{\frac{1}{2}}\frac{e}{\hbar c}(\epsilon_f-\epsilon_0)(\boldsymbol{\varepsilon}\cdot\mathbf{k})\times2\Big[\frac{2c+b}{q(a+b+c)}-\frac{b}{qa}+\frac{4c}{q^{\frac{3}{2}}}\tan^{-1}\frac{q^{\frac{1}{2}}}{2a+b}\Big](\chi_f{}^t,\chi_g{}^t),$$

$${}_0M_c{}^0=\Big(\frac{2\pi\hbar c}{\kappa V^2}\cdot\frac{2\pi\alpha}{1-\alpha r_{0t}}\Big)^{\frac{1}{2}}\frac{e}{\hbar c}(\epsilon_f-\epsilon_0)(\boldsymbol{\varepsilon}\cdot\mathbf{k})\frac{\hbar\kappa c}{\epsilon_0-\epsilon_f}\cdot\frac{\hbar\kappa}{2Mc}\Big[\frac{4a}{q^{\frac{3}{2}}}\tan^{-1}\frac{q^{\frac{1}{2}}}{2a+b}-\frac{2a+b}{q(a+b+c)}\Big](\chi_f{}^t,\chi_g{}^t),$$

$$\begin{aligned}{}_0M_{st}{}^0=&\Big(\frac{2\pi\hbar c}{\kappa V^2}\cdot\frac{2\pi\alpha}{1-\alpha r_{0t}}\Big)^{\frac{1}{2}}\frac{ie}{\hbar c}(\epsilon_f-\epsilon_0)\frac{\hbar\kappa c}{\epsilon_0-\epsilon_f}\cdot\frac{\hbar}{2Mc}\Big\{\frac{\mu_P}{\alpha^2+K_1{}^2}+\frac{\mu_n}{\alpha^2+K_2{}^2}\\ &-(\mu_P+\mu_n)\Big[\frac{(1-e^{i\delta_{0t}}\cos\delta_{0t})}{2k\kappa}\ln\Big(\frac{\alpha^2+K_1{}'^2}{\alpha^2+K_2{}'^2}\Big)\\ &-\frac{e^{i\delta_{0t}}\sin\delta_{0t}}{k\kappa}\tan^{-1}\frac{\alpha(K_1'-K_2')}{\alpha^2+K_1'K_2'}\\ &-\frac{e^{i\delta_{0t}}(k\cos\delta_{0t}+\alpha\sin\delta_{0t})}{k(\alpha^2+k^2)}\Big]\Big\}\\ &\times(\chi_f{}^t,\boldsymbol{\varepsilon}'\cdot(\boldsymbol{\sigma}_1+\boldsymbol{\sigma}_2)\chi_g{}^t),\end{aligned} \quad (10)$$

$$\begin{aligned}{}_0M_{ss}{}^0=&\Big(\frac{2\pi\hbar c}{\kappa V^2}\cdot\frac{2\pi\alpha}{1-\alpha r_{0t}}\Big)^{\frac{1}{2}}\frac{ie}{\hbar c}(\epsilon_f-\epsilon_0)\cdot\frac{\hbar\kappa c}{\epsilon_0-\epsilon_f}\\ &\cdot\frac{\hbar}{2Mc}\Big\{\frac{\mu_P}{\alpha^2+K_1{}^2}-\frac{\mu_n}{\alpha^2+K_2{}^2}\\ &-(\mu_P-\mu_n)\Big[\frac{(1-e^{i\delta_{0s}}\cos\delta_{0s})}{2k\kappa}\ln\Big(\frac{\alpha^2+K_1{}'^2}{\alpha^2+K_2{}'^2}\Big)\\ &-\frac{e^{i\delta_{0s}}\sin\delta_{0s}}{k\kappa}\tan^{-1}\frac{\alpha(K_1'-K_2')}{\alpha^2+K_1'K_2'}\Big]\Big\}\\ &\times(\chi_f{}^s,\boldsymbol{\varepsilon}'\cdot(\boldsymbol{\sigma}_1-\boldsymbol{\sigma}_2)\chi_g{}^t),\end{aligned}$$

where

$$\begin{aligned}&a=\alpha^2+k^2,\quad b=-\boldsymbol{\kappa}\cdot\mathbf{k},\quad c=\kappa^2/4,\quad q=4ac-b^2,\\ &\mathbf{K}_1=\mathbf{k}-\tfrac{1}{2}\boldsymbol{\kappa},\quad \mathbf{K}_2=\mathbf{k}+\tfrac{1}{2}\boldsymbol{\kappa},\\ &K_1'=k-\tfrac{1}{2}\kappa,\quad K_2'=k+\tfrac{1}{2}\kappa.\end{aligned} \quad (11)$$

The calculations involved in obtaining these matrix elements are, for the most part, straightforward. Some care is required in the calculation of ${}_0M_{st}{}^0$ inasmuch as long wavelength magnetic dipole transitions between

[12] J. Schwinger, Harvard Lecture Notes (unpublished).

the initial triplet S state and final triplet S state are forbidden due to the orthogonality of these two states. Since the wave functions used are not themselves orthogonal the forbiddenness of the transition was accounted for in the following way. We actually used in this calculation a modified $\mathfrak{M}_{st}$ interaction $\mathfrak{M}_{st}'$ that was obtained by subtracting from the $\mathfrak{M}_{st}$ interaction given in Sec. II a term obtained by expanding the exponential $\exp(i\boldsymbol{\kappa}\cdot\mathbf{r}/2)$ occurring in the $\mathfrak{M}_{st}$ interaction and retaining only the first term. That is,

$$\mathfrak{M}_{st}'=\mathfrak{M}_{st}-\left(\frac{2\pi\hbar c}{\kappa V}\right)^{\frac{1}{2}}\frac{ie}{\hbar c}(\epsilon_f-\epsilon_0)\frac{\hbar\kappa c}{\epsilon_0-\epsilon_f}\frac{\hbar}{Mc}\times\exp(i\boldsymbol{\kappa}\cdot\mathbf{R})[(\mu_P\tau_1{}^P+\mu_n\tau_1{}^n)\boldsymbol{\sigma}_1\cdot\boldsymbol{\varepsilon}'+(\mu_P\tau_2{}^P+\mu_n\tau_2{}^n)\boldsymbol{\sigma}_2\cdot\boldsymbol{\varepsilon}'].\quad(12)$$

In this way we have eliminated this dipole transition.

It will be noted that the calculated matrix elements of this first approximation are not dependent upon any assumed details of potential shape, and therefore, that the accuracy with which these results may be determined is limited only by the accuracy of the experimental results for the binding energy, triplet and singlet scattering lengths, and effective ranges. The integrations performed have been exact; thus the results of this approximation has been to give the matrix elements in an essentially zero-range approximation assuming half exchange, half ordinary force, to all multipole orders.

B. Approximation II-C

We will now investigate in detail the deviations from the results of Approximation I that may be expected when a particular form for a central force potential is chosen. We will consider in detail only the Hulthén potential since it is most amenable to calculation, and since previous calculations[5,6] seem to indicate that its results would differ very little from the results that would be obtained with other long-tailed potentials. We have repeated some of the calculations using a square well potential, with parameters obtained from the curves of Blatt and Jackson,[13] to correspond to the same effective range as our Hulthén potentials. These square well calculations were performed as a check and are, therefore, not described in detail. The results will be discussed in the consideration of the parallel Hulthén calculations.

Explicitly, the calculations in this section involve the modification $\psi_g{}^1$ of the ground-state wave function that is obtained because of our use here of the Hulthén potential $\mathfrak{U}_T(r)$. That is, with

$$\mathfrak{U}_t(r)=\frac{(\alpha^2-\beta^2)}{e^{(\beta-\alpha)r}-1}=(\alpha^2-\beta^2)\frac{e^{-\mu r}}{1-e^{-\mu r}},\quad\mu=\beta-\alpha,\quad(13)$$

we have

$$\psi_g{}^1=V^{-\frac{1}{2}}\exp(-i\boldsymbol{\kappa}\cdot\mathbf{R})\left[\frac{2\alpha}{4\pi(1-\alpha r_{0t})}\right]^{\frac{1}{2}}\times\left[\frac{e^{-\alpha r}-e^{-\beta r}}{r}-\frac{e^{-\alpha r}}{r}\right]2^{-\frac{1}{2}}(\xi_1\eta_2-\xi_2\eta_1)\chi_g{}^t,\quad(14)$$

where β is taken as $\beta=14.3\times10^{12}$ cm^{-1}, so that $\psi_g{}^1$ consists of only the difference between the Hulthén ground-state function and the shape-independent function used in Approximation I. In our modifications of the final-state S functions we keep in mind the fact that the transitions to the final singlet S state and to the final triplet P state are the dominant transitions since they correspond in the main to the magnetic and electric dipole transitions. In view of this the modification of the singlet final-state $\psi_{fs}{}^1$ is taken to represent only a modification of the final S state through the introduction of an *approximate* Hulthén final-state singlet S wave function. That is,

$$\psi_{fs}{}^1=V^{-1}2^{-\frac{1}{2}}[\xi_1\eta_2+\xi_2\eta_1]e^{-i\delta_{0s}}\left[\frac{(1-e^{-\eta r})}{kr}\sin(kr+\delta_{0s})-\frac{\sin(kr+\delta_{0s})}{kr}\right]\chi_f{}^s,\quad(15)$$

where η is taken as $\eta=12.8\times10^{12}$ cm^{-1}. The modification of the final triplet-state wave function takes account of interaction in the general final state through a Born approximation calculation in which the final plane wave is perturbed by the Hulthén potential. In particular, we are interested in the final triplet P state so that we will be concerned with the effect of varying the percentage of ordinary and exchange forces present in the potential, from the previously assumed Serber form. The modification of the final triplet wave function $\psi_{ft}{}^1$ is then (from the Born approximation)

$$\psi_{ft}{}^1=-V^{-1}(2\pi)^{-3}2^{-\frac{1}{2}}\times\left\{\xi_1\eta_2\int\int\frac{e^{i\mathbf{k}'\cdot(\mathbf{r}-\mathbf{r}')}}{k^2-k'^2}\mathfrak{U}_t(r')e^{i\mathbf{k}\cdot\mathbf{r}'}d\mathbf{k}'d\mathbf{r}'-\xi_2\eta_1\int\int\frac{e^{-i\mathbf{k}'\cdot(\mathbf{r}-\mathbf{r}')}}{k^2-k'^2}\times\mathfrak{U}_t(r')e^{-i\mathbf{k}\cdot\mathbf{r}'}d\mathbf{k}'d\mathbf{r}'\right\}\chi_f{}^t,\quad(16)$$

in which the nature of the force, exchange or ordinary, is still implicit in $\mathfrak{U}_t(r')$. For ease in performing the integrations indicated in (16) we have replaced the Hulthén potential by the corresponding Yukawa potential. That is, we have replaced $e^{-\mu r'}/(1-e^{-\mu r'})$ by $e^{-\mu r'}/\mu r'$. It will be noted that the modification of the final singlet state wave function does not include the possible effects of the variation of the percentage of charge exchange forces. This is consistent with the statement above that the dominant singlet final state

[13] J. M. Blatt and J. D. Jackson, Phys. Rev. **76**, 18 (1949).

is the S state where exchange force considerations have no effect.

As we have indicated above, it is well known that the electric and magnetic dipole interactions are by far the dominant effects for the energies we consider. Furthermore, it may be easily verified that the electric dipole interaction is included in $\mathcal{E}$ while the magnetic dipole interaction is included in $\mathfrak{M}_s$ (or alternatively $\mathfrak{M}_{ss}$). On this basis we expect that at these energies $\mathfrak{M}_c$ and $\mathfrak{M}_s$ employed with final triplet states (or alternatively $\mathfrak{M}_{st}$) will be relatively unimportant. The results of the numerical calculation of ${}_0M_c{}^0$ and ${}_0M_{st}{}^0$ bears this out. Therefore, in describing the effects of the wave function modification given above, we have restricted ourselves to the examination of only the E and M_{ss} matrix elements since it is clear that these will include all of the important effects. The matrix elements that we will calculate in this section are

$$\begin{gathered}{}_0E^1=(\psi_{ft}{}^0|\,\mathcal{E}\,|\psi_g{}^1), \qquad {}_1E^0=(\psi_{ft}{}^1|\,\mathcal{E}\,|\psi_g{}^0),\\ {}_1M_{ss}{}^0=(\psi_{fs}{}^1|\mathfrak{M}_s|\psi_g{}^0), \quad {}_0M_{ss}{}^1=(\psi_{fs}{}^0|\mathfrak{M}_s|\psi_g{}^1), \quad (17)\\ {}_1M_{ss}{}^1=(\psi_{fs}{}^1|\mathfrak{M}_s|\psi_g{}^1).\end{gathered}$$

We have not calculated ${}_1E^1$ since both ${}_1E^0$ and ${}_0E^1$ are themselves quite small, and this would represent a higher-order correction. On the other hand both ${}_1M_{ss}{}^0$ and ${}_0M_{ss}{}^1$ are rather large so that it was necessary to calculate ${}_1M_{ss}{}^1$. Since the forms of the integrals encountered in the three M_{ss} terms were essentially the same we have actually calculated the three terms together as one term that we will refer to as $M_{ss}{}^1$.

The results of the calculations for these matrix elements are

$${}_0E^1=-\left(\frac{2\pi\hbar c}{\kappa V^2}\cdot\frac{2\pi\alpha}{1-\alpha r_{0t}}\right)^{\frac{1}{2}}\frac{e}{\hbar c}(\epsilon_f-\epsilon_0)2\boldsymbol{\varepsilon}\cdot\mathbf{k}$$
$$\times\left[\frac{2c+b}{q'(a'+b+c)}-\frac{b}{q'a'}+\frac{4c}{q'^{\frac{3}{2}}}\tan^{-1}\frac{q'^{\frac{1}{2}}}{2a'+b}\right](\chi_f{}^t,\chi_g{}^t),$$

where $a'=\beta^2+k^2$, $q'=4a'c-b^2$.

$${}_1E^0=(-1)^v\left(\frac{2\pi\hbar c}{\kappa V^2}\cdot\frac{2\pi\alpha}{1-\alpha r_{0t}}\right)^{\frac{1}{2}}\frac{e}{\hbar c}(\epsilon_f-\epsilon_0)2\boldsymbol{\varepsilon}\cdot\mathbf{k}\frac{(\alpha^2-\beta^2)}{2\mu\kappa}$$
$$\times\left\{i\left[\frac{\mu^2+2k^2}{4k^2(\alpha^2+k^2)^2}\ln\frac{\mu^2+4k^2}{\mu^2}-\frac{1}{\alpha^2+k^2}\right]\right.$$
$$+\frac{\mu^2+2k^2}{2k^2(\alpha^2+k^2)^2}\left[\tan^{-1}\frac{2k\mu}{\mu^2-k^2-\alpha^2}-\tan^{-1}\frac{2k}{\mu}\right.$$
$$\left.-\tan^{-1}\frac{2\alpha k}{\mu^2+k^2-\alpha^2}\right]+\frac{\alpha^2-k^2}{2\alpha k(\alpha^2+k^2)^2}$$
$$+\frac{(\mu^2+k^2-\alpha^2)(\mu^2+k^2+\alpha^2)}{2\alpha k(\alpha^2+k^2)[(\mu^2+k^2-\alpha^2)^2+4\alpha^2k^2]}$$
$$\left.-\frac{(\mu^2+k^2-\alpha^2)}{2k^2(\alpha^2+k^2)}\cdot\frac{2\mu k}{(\mu^2-k^2-\alpha^2)^2+4\mu^2k^2}\right\}(\chi_f{}^t,\chi_g{}^t). \quad (18)$$

Here, $v=0$ for pure charge exchange forces and $v=1$ for ordinary forces. Also

$$M_{ss}{}^1=-\left(\frac{2\pi\hbar c}{\kappa V^2}\cdot\frac{2\pi\alpha}{1-\alpha r_{0t}}\right)^{\frac{1}{2}}\frac{ie}{\hbar c}(\epsilon_f-\epsilon_0)$$
$$\cdot\frac{\hbar\kappa c}{\epsilon_0-\epsilon_f}\cdot\frac{\hbar}{2Mc}\left\{\frac{\mu_P}{\beta^2+K_1{}^2}-\frac{\mu_n}{\beta^2+K_2{}^2}\right.$$
$$+\frac{(\mu_P-\mu_n)}{k\kappa}\left[\frac{(e^{i\delta_{0s}}\cos\delta_{0s}-1)}{2}\ln\left(\frac{\beta^2+K_1{}'^2}{\beta^2+K_2{}'^2}\right)\right.$$
$$+\frac{e^{i\delta_{0s}}}{2}\cos\delta_{0s}\ln\left\{\frac{[(\eta+\alpha)^2+K_1{}'^2][(\eta+\beta)^2+K_2{}'^2]}{[(\eta+\alpha)^2+K_2{}'^2][(\eta+\beta)^2+K_1{}'^2]}\right\}$$
$$+e^{i\delta_{0s}}\sin\delta_{0s}\left\{\tan^{-1}\frac{\beta(K_1'-K_2')}{\beta^2+K_1'K_2'}\right.$$
$$+\tan^{-1}\frac{(\eta+\alpha)(K_1'-K_2')}{(\eta+\alpha)^2+K_1'K_2'}$$
$$\left.\left.\left.-\tan^{-1}\frac{(\eta+\beta)(K_1'-K_2')}{(\eta+\beta)^2+K_1'K_2'}\right\}\right]\right\}$$
$$\times(\chi_f{}^s,\boldsymbol{\varepsilon}'\cdot(\boldsymbol{\sigma}_1-\boldsymbol{\sigma}_2)\chi_g{}^t).$$

The sums and averaging over spin states and polarizations have not yet been performed. It will be noted that in $M_{ss}{}^1$ one can easily separate out ${}_0M_{ss}{}^1$, ${}_1M_{ss}{}^0$, and ${}_1M_{ss}{}^1$ by referring to the constants β, η, and α. (That is, those terms which have β alone belong to ${}_0M_{ss}{}^1$, those terms involving η and α belong to ${}_1M_{ss}{}^0$, and those terms involving η and β belong to ${}_1M_{ss}{}^1$.)

In the calculation of ${}_1E^0$ another approximation was made, in addition to the use of the Yukawa form for the potential, in order that the contour integral involved be more tractable. We have not used in the calculation of this term the entire $\mathcal{E}$ interaction of Sec. II, but essentially only the dipole part that was obtained by expanding the exponential occurring in $\mathcal{E}$ and retaining only the first term. That is in $\mathcal{E}$, $[\tau_1{}^P\exp(is\boldsymbol{\kappa}\cdot\mathbf{r}/2)-\tau_2{}^P\exp(-is\boldsymbol{\kappa}\cdot\mathbf{r}/2)]$ was replaced by $\tau_1{}^P-\tau_2{}^P$. The error invoked by this simplification is very small since the term itself is quite small.

At this point we might indicate which square well calculations were performed, deferring the comparison of the two results to Sec. IV where the numerical results of the above calculations are given. We wished to check ${}_1E^0$ which at first sight appeared too small, and $M_{ss}{}^1$, which appeared too large. ${}_1E^0$ was compared to the result obtained using the formula[14] (45) of Marshall

[14] The formulas in the appendix of reference 6 are in error and should read

$$\tfrac{1}{2}M\ddot{x}_{01}=-(\partial V/\partial x)_{01}, \quad \ddot{x}_{01}=-(E_1-E_0)^2x_{01}/\hbar^2,$$
$$x_{01}=\frac{\hbar^2}{(E_0-E_1)^2}\int\psi_i\frac{\partial V}{\partial r}\cos\theta\psi_1d\tau,$$
$$\int\psi_i(\partial V/\partial r)\psi_ir^2dr=\psi_i(b_t)\psi_1(b_t)b_t{}^2V_0,$$

where V_0 is the depth of the square well. We believe that by use

and Guth for the matrix element with 100 percent ordinary force and using square well wave functions with the constants obtained from the curves of Blatt and Jackson so that the effective range was the same. $M_{ss}{}^1$ was compared to a straightforward magnetic dipole calculation in which the square well wave functions were used for both initial and final slates.

C. Approximation II-NC

The calculations treated in this section proceed in exactly the same manner as for Approximation II-C with central forces, with the obvious exception that where the explicit Hulthén central force potential and its associated wave functions occurred previously, it is understood that they are to be replaced by the appropriate noncentral terms. As before, we will calculate only the matrix elements, ${}_1E^0$, ${}_0E^1$, and $M_{ss}{}^1$ for exactly the same reasons as before. To distinguish between the results of these two second Approximations II, we will denote the matrix elements calculated here by ${}_0E_{NC}{}^1$, ${}_1E_{NC}{}^0$, and $M_{ss,NC}{}^1$.

It is not our intention, in this calculation with noncentral forces, to give a completely consistent result for the photodisintegration, but rather we intend merely to indicate the main effects of the introduction of the tensor force in the second Approximation. Thus, to fix the potential and wave functions, we nave not made any calculation of the electric quadrupole moment or magnetic moment of the deuteron, but instead we have chosen a potential and wave function that are probably reasonably correct and, at the same time, easily handled. The potential we have chosen is, in fact, somewhat more singular than is usually the case and, the wave functions we take for the ground state have been oversimplified. Explicitly, for the potential $\mathfrak{U}(\mathbf{r})$, we have taken[15]

$$\mathfrak{U}(\mathbf{r})=[1+\rho\{(\boldsymbol{\sigma}_1\cdot\nabla)(\boldsymbol{\sigma}_2\cdot\nabla)-\tfrac{1}{3}\boldsymbol{\sigma}_1\cdot\boldsymbol{\sigma}_2\nabla^2\}]\frac{(\alpha^2-\beta^2)e^{-\mu r}}{1-e^{-\mu r}},\quad(\mu=\beta-\alpha),\quad(19)$$

with the strength of the tensor portion $\rho=\mu^{-2}$. Indications are that this is about the right value for the strength.[16] It is a quite convenient choice, and in any event the numerical results are not very dependent upon this quantity.

In the modifications of the wave functions we have $\psi_{fs}{}^1$ and $\psi_{ft}{}^1$ of the same form as in the central force case. In $\psi_{ft}{}^1$ we must substitute the appropriate noncentral potential, and $\psi_{fs}{}^1$ remains exactly the same since the singlet potential remains central. For the ground-state wave function modification $\psi_g{}^1$ we now take

$$\psi_g{}^1=V^{-\frac{1}{2}}\exp(-i\boldsymbol{\kappa}\cdot\mathbf{R})\left(\frac{2\alpha}{4\pi(1-\alpha r_{0t})}\right)^{\frac{1}{2}}\times\left[u_{NC}(\mathbf{r})-\frac{e^{-\alpha r}}{r}\right]2^{-\frac{1}{2}}(\xi_1\eta_2-\xi_2\eta_1)\chi_g{}^t,\quad(20)$$

where

$$u_{NC}(\mathbf{r})=\left[1+(\tfrac{2}{5})^{-\frac{1}{2}}\times\left\{\frac{3(\boldsymbol{\sigma}_1\cdot\mathbf{r})(\boldsymbol{\sigma}_2\cdot\mathbf{r})}{r^2}-1\right\}\right]\frac{(e^{-\alpha r}-e^{-\beta r})}{r}.\quad(21)$$

The results for the calculations of the matrix elements, after integration but before the sums and averaging over spin states and polarizations have been performed, are

$$\begin{aligned}{}_0E_{NC}{}^1=&[1-(\tfrac{2}{5})^{-\frac{1}{2}}]{}_0E^1-(\tfrac{2}{5})^{-\frac{1}{2}}{}_0E^0\\&-\left(\frac{2\pi\hbar c}{\kappa V^2}\cdot\frac{2\pi\alpha}{1-\alpha r_{0t}}\right)^{\frac{1}{2}}\frac{e}{\hbar c}(\epsilon_f-\epsilon_0)\frac{3}{20}2^{-\frac{1}{2}}\\&\times\boldsymbol{\varepsilon}\cdot\nabla_k\times\left(\chi_f{}^t,\left\{[\sigma_1{}^x\sigma_2{}^xk_x+\sigma_1{}^y\sigma_2{}^yk_y\right.\right.\\&+\sigma_1{}^z\sigma_2{}^zk_z]\frac{2}{k^4}\left(\alpha\tan^{-1}\frac{k}{\alpha}-\beta\tan^{-1}\frac{k}{\beta}\right)\\&+(\boldsymbol{\sigma}_1\cdot\mathbf{k})(\boldsymbol{\sigma}_2\cdot\mathbf{k})\left[\frac{2}{k^4}\left(\frac{\alpha^2}{\alpha^2+k^2}-\frac{\beta^2}{\beta^2+k^2}\right)\right.\\&\left.\left.\left.-\frac{6}{k^5}\left(\alpha\tan^{-1}\frac{k}{\alpha}-\beta\tan^{-1}\frac{k}{\beta}\right)\right]\right\}\chi_g{}^t\right),\\{}_1E_{NC}{}^0=&[1-\rho\mu^2]{}_1E^0-(-1)^v\left(\frac{2\pi\hbar c}{\kappa V^2}\cdot\frac{2\pi\alpha}{1-\alpha r_{0t}}\right)^{\frac{1}{2}}\\&\times\frac{e}{\hbar c}(\epsilon_f-\epsilon_0)\frac{4}{3}\frac{\rho(\alpha^2-\beta^2)}{\mu^2}\\&\times\left(\chi_f{}^t,[(\boldsymbol{\sigma}_1\cdot\mathbf{k})(\boldsymbol{\sigma}_2\cdot\boldsymbol{\varepsilon})-(\boldsymbol{\sigma}_2\cdot\mathbf{k})(\boldsymbol{\sigma}_1\cdot\boldsymbol{\varepsilon})]\right.\\&\times\left\{\frac{\alpha(\mu^2k^2-\alpha^4+k^4)}{(\mu^2-\alpha^2-k^2)^2(\alpha^2+k^2)^2}\right.\\&-\frac{(\mu^2+k^2)^{\frac{3}{2}}}{2(\mu^2+2k^2)(\mu^2-\alpha^2+k^2)^2}\\&\left.\left.-\frac{ik^3}{2(\mu^2+2k^2)(\alpha^2+k^2)^2}\right\}\chi_g{}^t\right),\end{aligned}\quad(22)$$

of corrected formulas, the *large* difference found by Marshall and Guth for electric dipole cross sections with 50 percent ordinary −50 percent Majorana and with 100 percent ordinary forces, disappears.

[15] L. L. Foldy and R. E. Marshak, Phys. Rev. **75**, 1493 (1949); note added in proof.

[16] D. G. Padfield, Proc. Phys. Soc. (London) **A65**, 309 (1952).

$$M_{ss,NC}{}^{1}=[1-(\tfrac{2}{5})^{-\frac{1}{2}}]M_{ss}{}^{1}-(\tfrac{2}{5})^{-\frac{1}{2}}{}_{0}M_{ss}{}^{0}$$
$$+\left(\frac{2\pi\hbar c}{\kappa V^2}\cdot\frac{2\pi\alpha}{1-\alpha r_{0t}}\right)^{\frac{1}{2}}\frac{ie}{\hbar c}(\epsilon_f-\epsilon_0)$$
$$\times\frac{\hbar\kappa c}{\epsilon_0-\epsilon_f}\cdot\frac{\hbar}{2M_c}\frac{(\mu_P-\mu_n)}{20}2^{-\frac{1}{2}}$$
$$\times\left(\chi_f{}^{s},\boldsymbol{\varepsilon}'\cdot(\boldsymbol{\sigma}_1-\boldsymbol{\sigma}_2)\right\{3[\sigma_1{}^{x}\sigma_2{}^{x}k_x+\sigma_1{}^{y}\sigma_2{}^{y}k_y$$
$$+\sigma_1{}^{z}\sigma_2{}^{z}k_z]\frac{2}{k^4}\left(\beta\tan^{-1}\frac{k}{\beta}-\alpha\tan^{-1}\frac{k}{\alpha}\right)$$
$$+2(\boldsymbol{\sigma}_1\cdot\boldsymbol{\sigma}_2)\left[(e^{i\delta_{0s}}\cos\delta_{0s}-1)\left(\frac{1}{\alpha^2+k^2}-\frac{1}{\beta^2+k^2}\right)\right.$$
$$\left.\left.+\frac{e^{i\delta_{0s}}\sin\delta_{0s}}{k}\left(\frac{\alpha}{\alpha^2+k^2}-\frac{\beta}{\beta^2+k^2}\right)\right]\right\}\chi_g{}^{t}\Big).$$

In the above terms we have calculated in only the dipole approximation those integrals that involve the D-wave part of the ground-state wave function. That is, in those terms, we have used only the first term in the expansion of the exponential occurring in the $\mathcal{E}$ and $\mathfrak{M}_s$ interactions. This introduces no appreciable error and is consistent with the order of Approximation II.

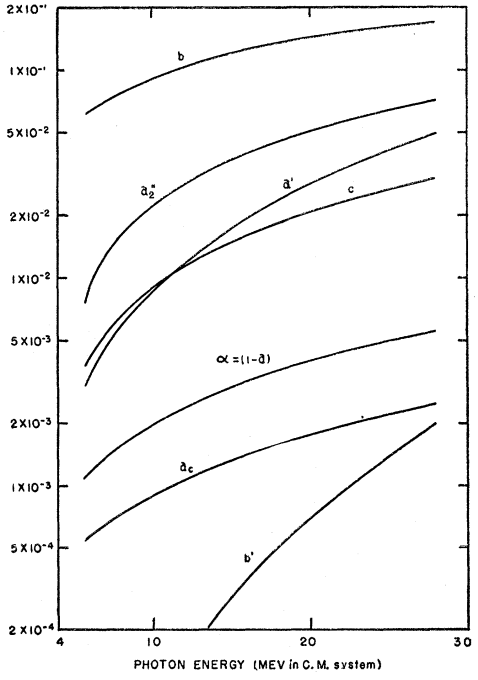

FIG. 1. Coefficients describing the departure from the matrix elements calculated in zero-range approximation in lowest multipole order due to our approximations and inclusion of all multipoles are plotted as a function of incident photon energy. The terms plotted here are those corresponding to ${}_0E^0$, ${}_1E^0$, ${}_0E^1$, and ${}_0M_c{}^0$. The form used is $(a+b\cos\theta+c\cos^2\theta)$ times the corresponding lowest multipole matrix element.

IV. RESULTS

The results of the calculations of the previous section are more easily interpreted if they are expressed in different form. The form we choose is to compare our results to the matrix elements that are obtained in the shape-independent theory using the lowest orders of the multipole expansion. Thus, we compare our E and M_c terms to the electric dipole matrix element, the M_{ss} terms are compared to the magnetic dipole matrix element, and the M_{st} term is compared to what is essentially the magnetic quadrupole matrix element. That is, we have written our results as the product of an appropriate multipole matrix element and a modifying expression composed of constants, for a given

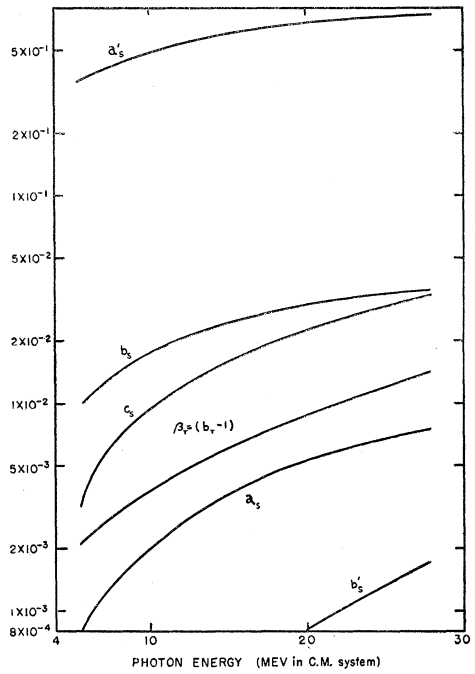

FIG. 2. The coefficients corresponding to ${}_0M_{ss}{}^0$, ${}_0M_{st}{}^0$, and $M_{ss}{}'$ are plotted in the same manner as for Fig. 1.

energy, and angular dependent terms. Then we may write for the central force matrix elements:

$${}_0E^0=\left(\frac{2\pi\hbar c}{\kappa V^2}\cdot\frac{2\pi\alpha}{1-\alpha r_{0t}}\right)^{\frac{1}{2}}\frac{e}{\hbar c}(\epsilon_f-\epsilon_0)2\boldsymbol{\varepsilon}\cdot\mathbf{k}$$
$$\times\frac{1}{(\alpha^2+k^2)^2}[a+b\cos\theta+c\cos^2\theta](\chi_f{}^{t},\chi_g{}^{t}),$$
$${}_0M_c{}^0=-\left(\frac{2\pi\hbar c}{\kappa V^2}\cdot\frac{2\pi\alpha}{1-\alpha r_{0t}}\right)^{\frac{1}{2}}\frac{e}{\hbar c}(\epsilon_f-\epsilon_0)2\boldsymbol{\varepsilon}\cdot\mathbf{k}$$
$$\times\frac{1}{(\alpha^2+k^2)^2}[a_c+b_c\cos\theta+c_c\cos^2\theta](\chi_f{}^{t},\chi_g{}^{t}),$$

$$
{}_0M_{st}{}^0=\left(\frac{2\pi\hbar c}{\kappa V^2}\cdot\frac{2\pi\alpha}{1-\alpha r_{0t}}\right)^{\frac{1}{2}}\frac{ie}{\hbar c}(\epsilon_f-\epsilon_0)
\times\frac{\hbar\kappa c}{(\epsilon_0-\epsilon_f)}\frac{\hbar}{2Mc}(\mu_P+\mu_n)\frac{\boldsymbol{\kappa}\cdot\mathbf{k}}{(\alpha^2+k^2)^2}
\times[b_t+c_t\cos\theta](\chi_f{}^t,\boldsymbol{\varepsilon}'\cdot(\boldsymbol{\sigma}_1+\boldsymbol{\sigma}_2)\chi_g{}^t),
$$

$$
{}_0M_{ss}{}^0=\left(\frac{2\pi\hbar c}{\kappa V^2}\cdot\frac{2\pi\alpha}{1-\alpha r_{0t}}\right)^{\frac{1}{2}}\frac{ie}{\hbar c}(\epsilon_f-\epsilon_0)
\times\frac{\hbar\kappa c}{(\epsilon_0-\epsilon_f)}\frac{\hbar}{2Mc}\frac{(\mu_P-\mu_n)}{(\alpha^2+k^2)}\left[\cos\delta_{0s}+\frac{\alpha}{k}\sin\delta_{0s}\right] \quad (23)
$$

$$
\times[e^{i\delta_{0s}}-a_s+b_s\cos\theta+c_s\cos^2\theta]
\times(\chi_f{}^s,\boldsymbol{\varepsilon}'\cdot(\boldsymbol{\sigma}_1-\boldsymbol{\sigma}_2)\chi_g{}^t),
$$

$$
{}_0E'=-\left(\frac{2\pi\hbar c}{\kappa V^2}\cdot\frac{2\pi\alpha}{1-\alpha r_{0t}}\right)^{\frac{1}{2}}\frac{e}{\hbar c}(\epsilon_f-\epsilon_0)2\boldsymbol{\varepsilon}\cdot\mathbf{k}
\times\frac{1}{(\alpha^2+k^2)^2}[a'+b'\cos\theta](\chi_f{}^t,\chi_g{}^t),
$$

$$
{}_1E^0=(-1)^v\left(\frac{2\pi\hbar c}{\kappa V^2}\cdot\frac{2\pi\alpha}{1-\alpha r_{0t}}\right)^{\frac{1}{2}}\frac{e}{\hbar c}(\epsilon_f-\epsilon_0)2\boldsymbol{\varepsilon}\cdot\mathbf{k}
\times\frac{1}{(\alpha^2+k^2)^2}[a_1''+ia_2'']({\chi_f}^t,\chi_g{}^t),
$$

$$
M_{ss}'=-\left(\frac{2\pi\hbar c}{\kappa V^2}\cdot\frac{2\pi\alpha}{1-\alpha r_{0t}}\right)\frac{ie}{\hbar c}(\epsilon_f-\epsilon_0)
\times\frac{\hbar\kappa c}{(\epsilon_0-\epsilon_f)}\frac{\hbar}{2Mc}\frac{(\mu_P-\mu_N)}{(\alpha^2+k^2)}\left[\cos\delta_{0s}+\frac{\alpha}{k}\sin\delta_{0s}\right]
\times[a_s'e^{i\delta_{0s}}+b_s'\cos\theta](\chi_f{}^s,\boldsymbol{\varepsilon}'\cdot(\boldsymbol{\sigma}_1-\boldsymbol{\sigma}_2)\chi_g{}^t).
$$

Thus the results of our calculations are readily evident from the magnitudes of the coefficients of the angular terms. These coefficients are plotted against the incident gamma-ray energy in Figs. 1, 2, and 3.

In the expressions above it is clear that the expressions of the form $(a+b\cos\theta+c\cos^2\theta)$ demonstrate the effects of the additional consideration we have made; i.e., higher multipoles, explicit Hulthén shape, and interaction in the final states. The remaining factor of the terms are, in the case of ${}_0E^0$, ${}_0M_c{}^0$, ${}_0E^1$, and ${}_1E^0$ the electric dipole matrix element between the shape-independent ground-state function $\psi_g{}^0$ and the free-particle final triplet P-state function. In the case of ${}_0M_{ss}{}^0$ and $M_{ss}{}^1$, the remainder is the magnetic dipole matrix element between the shape-independent ground-state wave function $\psi_g{}^0$ and the final singlet S-state wave function in which a correction for interaction has been introduced by means of the phase shift. Both of these cases may be easily obtained from our interaction by using only the first term of the expansion for the exponentials occurring in the $\mathcal{E}$ and $\mathfrak{M}_s$ interactions. This is just what we have been calling the dipole approximation for our interaction. The remainder in the ${}_0M_{st}{}^0$ expression has been obtained by replacing, in the original calculation of ${}_0M_{st}{}^0$, the exponential occurring in the $\mathfrak{M}_{st}$ interaction by the second term of its expansion. This is the analogous term to the magnetic quadrupole term. The coefficients of the angular terms in the modifying expression were arrived at in the following way. The original expressions, Eqs. (10) and (18), for the different matrix elements were numerically calculated at five energies in the range from 5 Mev to 30 Mev, i.e., 5.66 Mev, 11.23, 16.53, 22.44, and 28.06 Mev, and for seven angles at each energy; i.e., 0°, 30°, 60°, 90°, 120°, 150°, and 180°. For each energy the results for each matrix element were numerically fitted to the corresponding term of the above expressions, Eqs. (23), in this way obtaining the coefficients. In all cases these expressions represent the calculated terms to better than one percent at all angles. The coefficients thus obtained were then plotted as a function of the incident gamma-ray energy in Figs. 1, 2, and 3. Actually, only those coefficients whose effects are noticeable are plotted. Higher-order terms in such an expansion in powers of the cosine than those given are at least an order of magnitude smaller than the smallest of the terms given.

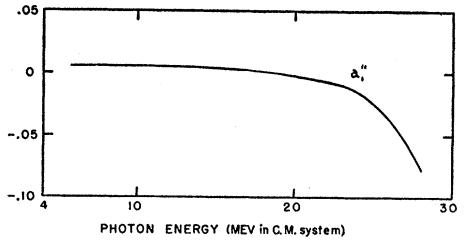

FIG. 3. A term corresponding to ${}_1E^0$ is plotted in the same manner as in Fig. 1.

Referring to these curves and Eqs. (23), it will be observed that the first coefficient in the modifying expression for each matrix element is the dominant term. This is expected since the more complicated angular behaviour corresponds to the higher multipoles. These first coefficients in the cases of ${}_0E^0$ and ${}_0M_{st}{}^0$ are very nearly equal to unity so that in these cases we have plotted their departures from unity, i.e., for a we plot $\alpha=1-a$, for b_t we plot $\beta_t=b_t-1$. The first coefficients of ${}_0E^1$ and ${}_0M_c{}^0$, a^1 and a_c, respectively, are as expected much smaller although still not negligible because they will interfere with ${}_0E^0$. The term of importance in ${}_1E^0$, that is, a_1'', is smaller than had been anticipated, but this result has been corroborated by an alternative calculation using the method of Marshall and Guth[14] for calculating the electric dipole matrix element with 100 percent ordinary forces and using square well wave

functions. The agreement was excellent at our higher energies, above 15 Mev, and was in very good qualitative agreement at the lower energies where the Born approximation is not as good. Similarly, the term in M_{ss}', a_s', was larger than was expected and this was checked by a magnetic dipole calculation using square well wave functions described previously. At the lowest energy for which we calculated, the agreement is excellent while at our higher energies the agreement is is within 10 percent of the calculated correction term.

The second and third terms in the modifying expressions reflect the presence of the higher multipoles. It is evident that though these terms are small they will not be negligible in their effects on the angular distribution, even at our lowest energies. This is more clearly seen by writing the differential cross section for the photodisintegration in terms of these coefficients. It is to be understood that by the Approximation II-C cross section we mean the calculated cross section in which the second Approximation terms are included. Obviously, the first Approximation terms are also included. Thus, we have for the differential cross section in the second Approximation with central forces, and for an unpolarized γ-ray beam:

$$\frac{d\Omega_{\mathrm{II}}}{d\Omega}=\frac{M}{2\hbar^2}\frac{e^2}{\hbar^2c^2}\frac{\alpha}{1-\alpha r_{0t}}(\epsilon_f-\epsilon_0)^2\frac{k}{\kappa}\Big\{\frac{2k^2\sin^2\theta}{(\alpha^2+k^2)^4}$$
$$\times[(a-a'-a_c+(-1)^v a_1'')$$
$$+(b-b')\cos\theta+c\cos^2\theta]^2$$
$$+\Big[\frac{\hbar\kappa c}{(\epsilon_0-\epsilon_f)}\frac{\hbar}{2Mc}\frac{(\mu_P-\mu_n)}{(\alpha^2+k^2)}\Big]^2\Big[\Big(\cos\delta_{0s}+\frac{\alpha}{k}\sin\delta_{0s}\Big)^2$$
$$\times\frac{4}{3}[(1-a_s')e^{i\delta_{0s}}-a_s+(b_s-b_s')\cos\theta+c_s\cos^2\theta]^2$$
$$+\frac{k^2\kappa^2}{(\alpha^2+k^2)^4}\cos^2\theta\cdot\frac{8}{3}b_t^2\Big]\Big\}, \quad (24)$$

where θ is the angle between the direction of the incident γ ray and the emergent proton.

The differential cross section in Approximation I, $d\sigma_{\mathrm{I}}/d\Omega$, is easily obtained from the above expression Approximation II by simply omitting a', a_1'', a_s', b_s' where they occur. It is not convenient to express the differential cross section obtained from Approximation II-NC in the above form because of the more complicated spin dependence of the matrix elements. This results in a greater degree of interference between the different terms entering in the calculation of the cross section. For a similar reason we have not felt it particularly illuminating to express the noncentral case matrix elements in the form of Eqs. (23) either. However, in discussing the numerical results for the angular distribution of the different differential cross sections it is more convenient to write the differential cross section in the form

$$d\sigma/d\Omega=A+B\sin^2\theta+C\sin^2\theta\cos\theta$$
$$+D\sin^2\theta\cos^2\theta+E\sin^4\theta\cos\theta, \quad (25)$$

and this form applies equally well for the noncentral as well as central force cases.

The angular distribution is then easily described in terms of the ratio of each of the other coefficients to B, where B is the dominant term corresponding in the main to the electric dipole contribution. Thus A/B gives the measure of the isotropy in the angular distribution, C/B and E/B measure the forward asymmetry, and D/B measures the broadening of the peak of the angular distribution. These ratios are plotted as a function of incident γ-ray energy in the center-of-mass system for the three cases in Fig. 4. The subscript I refers to the quantities in Approximation I, II to the Approximation II-C cross-section, and N.C. to Approximation II-NC. E/B is plotted in only the case of Approximation II-NC since it is only in this case that it is appreciable.

The resultant total cross section can, of course, be written as

$$\sigma=4\pi[A+\tfrac{2}{3}B+(2/15)D]. \quad (26)$$

The calculated total cross sections are given in Figs. 5 and 6 as a function of incident gamma-ray energy. In Fig. 5 three curves appear, one for σ_{I}, the result from Approximation I, for σ_{II} (50 percent), the result from Approximation II with central forces that are 50 percent charge-exchange, 50 percent ordinary, and for $\sigma_{\mathrm{N.C.}}$, the result of Approximation II-N.C. with forces that are

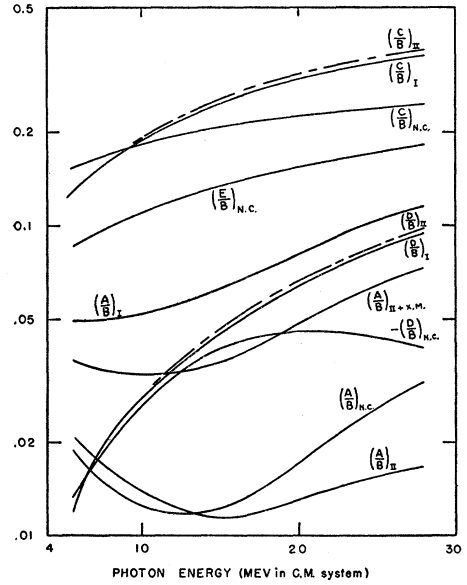

FIG. 4. The angular dependence of the differential cross sections in the three approximations I, II, and IINC, and including the effects of exchange moments in II+X.M. is plotted as a function of incident photon energy. The form assumed for the cross section is $d\sigma/d\Omega=A+B\sin^2\theta+C\sin^2\theta\cos\theta+D\sin^2\theta\cos^2\theta+E\sin^4\theta\cos\theta$.

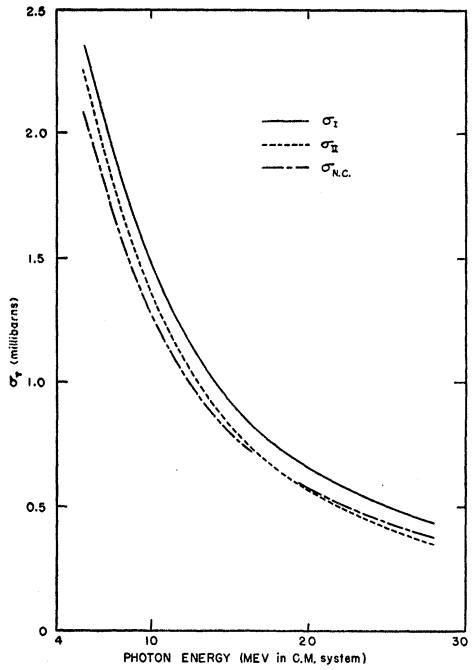

FIG. 5. The total cross section in millibarns is plotted as a function of the incident photon energy for the three approximations calculated, I, II, and IINC.

50 percent charge exchange, and 50 percent ordinary. In Fig. 6, we have plotted the case of Approximation II-C with central forces and 0 percent charge exchange forces, $\sigma_{II}(0 \text{ percent})$, in the form of the ratio $\sigma_{II}(0 \text{ percent})/\sigma_{II}(50 \text{ percent})$ of this cross section to the cross section from Approximation II-C with central forces, and 50 percent charge exchange which appears in Fig. 5. From the curves of the differential and total cross sections, Figs. 4, 5, and 6 and the appropriate equations, (25) and (26), it is clear that the values of the coefficients A, B, C, D, and E may easily be obtained for each case and for any of the energies in the range calculated.

V. EXCHANGE-MOMENT CONTRIBUTION

In the preceding sections we have not treated the interaction due to exchange currents in the deuteron, arising from the charge-exchange character of nuclear forces, even though it is to be expected that such effects are present, because the explicit form for the interaction must depend upon the choice of meson theory to be used. In the absence of a suitable meson theory, it is, however, still possible to obtain some information from a phenomenological approach. In a recent paper[10] such a phenomenological method was described, in which, on the basis of differential charge conservation and reasonable symmetry restrictions on the nuclear Hamiltonian, consideration was given to the possible operational forms for the two-body exchange current operators. The resultant magnetic moment operators were obtained which, for convenience, we will list again here. They are, for general nuclei:

$$\mathbf{M}_l=(e/4\hbar c)\sum_{i\neq j}V_{ij}(\tau_i^x\tau_j^y-\tau_i^y\tau_j^x)[\mathbf{x}_i\times\mathbf{x}_j],$$

$$\mathbf{M}_{\mathrm{I}}=\tfrac{1}{4}\sum_{i<j}F_{\mathrm{I}}(r_{ij})(\tau_i^x\tau_j^y-\tau_i^y\tau_j^x)(\boldsymbol{\sigma}_i\times\boldsymbol{\sigma}_j),$$

$$\mathbf{M}_{\mathrm{I}'}=\tfrac{1}{4}\sum_{i<j}F_{\mathrm{I}'}(r_{ij})(\tau_i^x\tau_j^y-\tau_i^y\tau_j^x)\times\{3[\mathbf{r}_{ij}\cdot(\boldsymbol{\sigma}_i\times\boldsymbol{\sigma}_j)]\mathbf{r}_{ij}/r_{ij}^2-(\boldsymbol{\sigma}_i\times\boldsymbol{\sigma}_j)\},$$

$$\mathbf{M}_{\mathrm{II}}=\tfrac{1}{4}\sum_{i<j}F_{\mathrm{II}}(r_{ij})(\tau_i^z-\tau_j^z)(\boldsymbol{\sigma}_i-\boldsymbol{\sigma}_j),$$

$$\mathbf{M}_{\mathrm{II}'}=\tfrac{1}{4}\sum_{i<j}F_{\mathrm{II}'}(r_{ij})(\tau_i^z-\tau_j^z)\times\{3[\mathbf{r}_{ij}\cdot(\boldsymbol{\sigma}_i-\boldsymbol{\sigma}_j)]\mathbf{r}_{ij}/r_{ij}^2-(\boldsymbol{\sigma}_i-\boldsymbol{\sigma}_j)\},$$

$$\mathbf{M}_{\mathrm{III}}=\tfrac{1}{4}\sum_{i<j}F_{\mathrm{III}}(r_{ij})(\tau_i^z+\tau_j^z)(\boldsymbol{\sigma}_i+\boldsymbol{\sigma}_j),$$

$$\mathbf{M}_{\mathrm{III}'}=\tfrac{1}{4}\sum_{i<j}F_{\mathrm{III}'}(r_{ij})(\tau_i^z+\tau_j^z)\times\{3[\mathbf{r}_{ij}\cdot(\boldsymbol{\sigma}_i+\boldsymbol{\sigma}_j)]\mathbf{r}_{ij}/r_{ij}^2-(\boldsymbol{\sigma}_i+\boldsymbol{\sigma}_j)\},\quad(27)$$

$$\mathbf{M}_{\mathrm{IV}}=\tfrac{1}{4}\sum_{i<j}F_{\mathrm{IV}}(r_{ij})(1+\tau_i^z\tau_j^z)(\boldsymbol{\sigma}_i+\boldsymbol{\sigma}_j),$$

$$\mathbf{M}_{\mathrm{IV}'}=\tfrac{1}{4}\sum_{i<j}F_{\mathrm{IV}'}(r_{ij})(1+\tau_i^z\tau_j^z)\times\{3[\mathbf{r}_{ij}\cdot(\boldsymbol{\sigma}_i+\boldsymbol{\sigma}_j)]\mathbf{r}_{ij}/r_{ij}^2-(\boldsymbol{\sigma}_i+\boldsymbol{\sigma}_j)\},$$

$$\mathbf{M}_{\mathrm{V}}=\tfrac{1}{4}\sum_{i<j}F_{\mathrm{V}}(r_{ij})(1-\tau_i^z\tau_j^z)(\boldsymbol{\sigma}_i+\boldsymbol{\sigma}_j),$$

$$\mathbf{M}_{\mathrm{V}'}=\tfrac{1}{4}\sum_{i<j}F_{\mathrm{V}'}(r_{ij})(1-\tau_i^z\tau_j^z)\times\{3[\mathbf{r}_{ij}\cdot(\boldsymbol{\sigma}_i+\boldsymbol{\sigma}_j)]\mathbf{r}_{ij}/r_{ij}^2-(\boldsymbol{\sigma}_i+\boldsymbol{\sigma}_j)\},$$

$$\mathbf{M}_{\mathrm{VI}}=-\tfrac{1}{4}\sum_{i<j}F_{\mathrm{VI}}(r_{ij})(\tau_i^x\tau_j^x+\tau_i^y\tau_j^y)(\boldsymbol{\sigma}_i+\boldsymbol{\sigma}_j),$$

$$\mathbf{M}_{\mathrm{VI}'}=-\tfrac{1}{4}\sum_{i<j}F_{\mathrm{VI}'}(r_{ij})(\tau_i^x\tau_j^x+\tau_i^y\tau_j^y)\times\{3[\mathbf{r}_{ij}\cdot(\boldsymbol{\sigma}_i+\boldsymbol{\sigma}_j)]\mathbf{r}_{ij}/r_{ij}^2-(\boldsymbol{\sigma}_i+\boldsymbol{\sigma}_j)\},$$

with the general expression for the magnetic moment operator of the nuclear system being

$$\mathbf{M}=\mathbf{M}_l+\textstyle\sum_N C_N\mathbf{M}_N,\quad(28)$$

where the C_N are arbitrary constants.

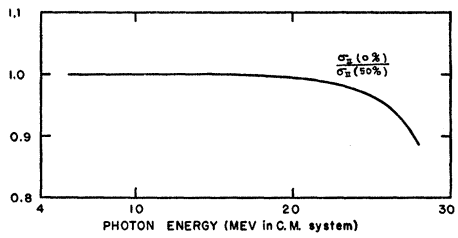

FIG. 6. The ratio of the total cross section calculated in Approximation II with 100 percent ordinary forces to the total cross section calculated in Approximation II with 50 percent charge-exchange forces (which appears in Fig. 5) is plotted as a function of incident photon energy.

We see that aside from $\mathbf{M}_l$, the remaining twelve exchange-moment operators $M_{\mathrm{I}}-M_{\mathrm{VI}'}$ have within them an arbitrary function of r_{ij}, the separation of the ith and jth nucleons. It was there assumed that all twelve of these functions were the same and of the form of a Gaussian function. Choosing a reasonable value for the range of the Gaussian it was then possible, by referring to the experimental data on the magnetic moment anomalies of the deuteron, triton, He^3, and heavy odd nuclei, to obtain some information on the values of the multiplicative constants C_N which represent the strengths of the different terms. It is our purpose to utilize these numerical results for estimating the magnitude of the contribution of exchange moment effects on the matrix elements for photodisintegration in the magnetic dipole approximation.

For the deuteron it may readily be verified that the exchange moment operators $\mathbf{M}_l$, $\mathbf{M}_{\mathrm{III}}$, $\mathbf{M}_{\mathrm{III}'}$, $\mathbf{M}_{\mathrm{IV}}$, and $\mathbf{M}_{\mathrm{IV}'}$ can give no contribution to the matrix elements for photodisintegration. $\mathbf{M}_l$ cannot contribute for any two-nucleon system, while the other four terms have a null contribution because the deuteron has a singlet isotopic spin ground-state wave function which, when operated upon by the isotopic spin operator parts of $\mathbf{M}_{\mathrm{III}}$, $\mathbf{M}_{\mathrm{III}'}$, $\mathbf{M}_{\mathrm{IV}}$, and $\mathbf{M}_{\mathrm{IV}'}$, yields zero identically. If we assume that the ground state of the deuteron is completely an S state, as we shall in this calculation, the selection rules for the remainder of the exchange moment operators may readily be obtained. Thus $\mathbf{M}_{\mathrm{I}}$ and $\mathbf{M}_{\mathrm{II}}$ give rise to transitions to a final singlet S state, while $\mathbf{M}_{\mathrm{I}'}$ and $\mathbf{M}_{\mathrm{II}'}$ give rise to transitions to final singlet S or singlet D states. $\mathbf{M}_{\mathrm{V}}$ and $\mathbf{M}_{\mathrm{VI}}$ give rise to transitions to final triplet S states, while $\mathbf{M}_{\mathrm{V}'}$ and $\mathbf{M}_{\mathrm{VI}'}$ may give rise to transitions to either final triplet S or triplet D states in the deuteron.

Since $\mathbf{M}_{\mathrm{V}}$, $\mathbf{M}_{\mathrm{V}'}$, $\mathbf{M}_{\mathrm{VI}}$, and $\mathbf{M}_{\mathrm{VI}'}$ would give exchange contributions to the magnetic moment of the deuteron, the conclusion arrived at was that the strengths of these terms are probably very small. On the other hand, the strengths of $\mathbf{M}_{\mathrm{I}}$, $\mathbf{M}_{\mathrm{I}'}$, $\mathbf{M}_{\mathrm{II}}$, and $\mathbf{M}_{\mathrm{II}'}$ may be quite a bit larger, by at least an order of magnitude. For our purpose of merely estimating the magnitudes of these contributions to the photodisintegration it will be sufficient to consider only the terms $\mathbf{M}_{\mathrm{I}}$, $\mathbf{M}_{\mathrm{I}'}$, $\mathbf{M}_{\mathrm{II}}$, $\mathbf{M}_{\mathrm{II}'}$. That is, for the deuteron we consider

$$\begin{aligned}
&C_{\mathrm{I}}\mathbf{M}_{\mathrm{I}}=\tfrac{1}{4}C_{\mathrm{I}}f(r)(\tau_1{}^x\tau_2{}^y-\tau_1{}^y\tau_2{}^x)(\boldsymbol{\sigma}_1\times\boldsymbol{\sigma}_2),\\
&C_{\mathrm{I}'}\mathbf{M}_{\mathrm{I}'}=\tfrac{1}{4}C_{\mathrm{I}'}f(r)(\tau_1{}^x\tau_2{}^y-\tau_1{}^y\tau_2{}^x)\\
&\qquad\times\{3[\mathbf{r}\cdot(\boldsymbol{\sigma}_1\times\boldsymbol{\sigma}_2)]\mathbf{r}/r^2-(\boldsymbol{\sigma}_1\times\boldsymbol{\sigma}_2)\},\\
&C_{\mathrm{II}}\mathbf{M}_{\mathrm{II}}=\tfrac{1}{4}C_{\mathrm{II}}f(r)(\tau_1{}^z-\tau_2{}^z)(\boldsymbol{\sigma}_1-\boldsymbol{\sigma}_2),\\
&C_{\mathrm{II}'}\mathbf{M}_{\mathrm{II}'}=\tfrac{1}{4}C_{\mathrm{II}'}f(r)(\tau_1{}^z-\tau_2{}^z)\\
&\qquad\times\{3[\mathbf{r}\cdot(\boldsymbol{\sigma}_1-\boldsymbol{\sigma}_2)]\mathbf{r}/r^2-(\boldsymbol{\sigma}_1-\boldsymbol{\sigma}_2)\}.
\end{aligned}\tag{29}$$

In our calculations we will assume for simplicity that $C_{\mathrm{I}}=3C_{\mathrm{I}'}$ and $C_{\mathrm{II}}=3C_{\mathrm{II}'}$, and we will choose for $f(r)$ a Hulthén form rather than a Gaussian, although this causes some further uncertainty in the values of the coefficients. That is, we choose

$$f(r)=e^{-\mu r}/(1-e^{-\mu r}).\tag{30}$$

For the ground-state wave function ψ_g we take

$$\psi_g=\frac{1}{\sqrt{V}}\exp(-i\boldsymbol{\kappa}\cdot\mathbf{R})\left(\frac{2\alpha}{4\pi(1-\alpha r_{0t})}\right)^{\frac{1}{2}}\times\frac{(e^{-\alpha r}-e^{-\beta r})}{r}\frac{1}{\sqrt{2}}(\xi_1\eta_2-\xi_2\eta_1)\chi_g{}^t,\tag{31}$$

and for the final state we need only consider the final singlet-state wave function ψ_{fs}, where

$$\psi_{fs}=\frac{1}{\sqrt{2V^2}}\left\{\xi_1\eta_2e^{i\mathbf{k}\cdot\mathbf{r}}+\xi_2\eta_1e^{-i\mathbf{k}\cdot\mathbf{r}}-[\xi_1\eta_2+\xi_2\eta_1]\left[\frac{\sin kr}{kr}-\frac{e^{-i\delta_{0s}}\sin(kr+\delta_{0s})}{kr}\right]\right\}\chi_f{}^s.\tag{32}$$

The results for the matrix elements are the same for $\mathbf{M}_{\mathrm{I}}$ and $\mathbf{M}_{\mathrm{II}}$ as well as for $\mathbf{M}_{\mathrm{I}'}$ and $\mathbf{M}_{\mathrm{II}'}$. Thus, before the summation and averaging over spin states and polarizations we have

$$\begin{aligned}
&(\psi_f|C_{\mathrm{I}}(M_{\mathrm{I}}+M_{\mathrm{I}'})|\psi_g)=(\psi_f|C_{\mathrm{II}}(M_{\mathrm{II}}+M_{\mathrm{II}'})|\psi_g)\\
&=\left(\frac{2\pi\hbar c}{\kappa V^2}\cdot\frac{2\pi\alpha}{1-\alpha r_{0t}}\right)^{\frac{1}{2}}\frac{e}{2\hbar c}(\epsilon_f-\epsilon_0)\frac{\hbar\kappa c}{(\epsilon_0-\epsilon_f)}\frac{\hbar}{Mc}2C_N\\
&\times\chi_f{}^s\left\{\boldsymbol{\varepsilon}'\cdot\mathbf{S}_N\left[\frac{e^{-i\delta_{0s}}}{\beta^2+k^2}\left(\cos\delta_{0s}+\beta/k\,\sin\delta_{0s}-\frac{e^{i\delta_{0s}}}{4}\right)\right]\right.\\
&+\frac{\boldsymbol{\varepsilon}'\cdot\mathbf{k}}{k^2}(\mathbf{S}_N\cdot\mathbf{k})\left[\frac{1}{k^2}\left(\frac{2+k^2/\beta^2}{1+k^2/\beta^2}\right)+\frac{1}{k^2}-\frac{3\beta}{k^3}\tan^{-1}\frac{k}{\beta}\right]\\
&\left.+\frac{(\epsilon_x'S_{Nx}k_x+\epsilon_y'S_{Ny}k_y)}{k}\left[\frac{\beta}{k^3}\tan^{-1}\frac{k}{\beta}-\frac{1}{k^2}\right]\right\}\chi_g{}^t,
\end{aligned}\tag{33}$$

where C_N is either C_{I} or C_{II}, and S_N is the corresponding spin operator, $\mathbf{S}_{\mathrm{I}}=(\boldsymbol{\sigma}_1\times\boldsymbol{\sigma}_2)$ and $\mathbf{S}_{\mathrm{II}}=(\boldsymbol{\sigma}_1-\boldsymbol{\sigma}_{\mathrm{II}})$; however, $\mathbf{S}_{\mathrm{I}}$ and $\mathbf{S}_{\mathrm{II}}$ have exactly the same effects operating on the deuteron ground-state triplet spin function $\chi_g{}^t$.

The original calculations[10] to determine the magnitudes of the C_N's performed with a Gaussian for $f(r)$ indicated magnitudes for C_{I} and C_{II} of the order of a nuclear magneton. We have estimated the effect on the C_N's of the use of the Hulthén form for $f(r)$ instead of the Gaussian by two methods. The first consisted of equating the expectation values for the magnetic moment of the deuteron for the two forms, and the second consisted of normalizing both interaction forms to the same volume and then equating them. Neither method is completely satisfactory but both methods do indicate that the constants, i.e., strengths, to be used with the Hulthén form should be somewhat larger than those

obtained by using the Gaussian. We have chosen as a conservative estimate the relation

$$C_{\mathrm{I}}+C_{\mathrm{II}}=2.0 \text{ nm} \tag{34}$$

to serve as our basis for estimating the exchange moment effect on the photodisintegration. Though, of course, inexact, this value should be of the correct order of magnitude to indicate the possible extent of the influence of the exchange moments.

The resulting contribution to the photodisintegration matrix element interferes with the contributions of the $\mathfrak{M}_{ss}$ interaction. Despite the complicated form of the matrix elements the main part of the contribution is isotropic, and, in fact, the angular dependent part may be ignored. The contribution of the exchange moment terms to the differential cross section is indicated in Fig. 4 by the plot of $(A/B)_{\mathrm{II+XM}}$. This quantity was obtained by adding the exchange-moment contribution, considered as completely isotropic, to the matrix elements of Approximation II with central forces, thus yielding a new differential cross section to which this quantity refers. The magnitude of the exchange-moment contribution is indicated by comparison of $(A/B)_{\mathrm{II+XM}}$ to the quantity $(A/B)_{\mathrm{II}}$. The contribution of the exchange moments to the total cross section is indicated in Fig. 7 where the difference between the total cross section given by Approximation II with central forces and 50 percent charge exchange with the inclusion of the exchange moment and the quantity σ_{II} (50 percent) without the exchange-moment contribution is plotted as a function of the incident gamma-ray energy.

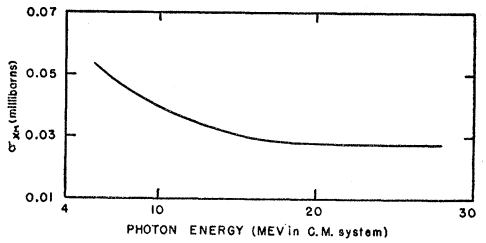

FIG. 7. The contribution to the total cross section due to the inclusion of exchange moments is plotted as a function of incident photon energy. σ_{XM} is the difference between the cross section given by Approximation II with 50 percent charge-exchange forces and including the exchange moments and the same Approximation without the exchange moments.

VI. DISCUSISON OF RESULTS

All of the salient results of this paper are summarized in the Figs. 1 through 7. In this section we will discuss these results in the order in which we have presented them.

A. Approximation I

The results obtained in Approximation I are characterized by the curves for α, b, c, a_c, β_t, a_s, b_s, and c_s in Figs. 1 and 2 which describe the behavior of the matrix elements; the curves for $(A/B)_{\mathrm{I}}$, $(C/B)_{\mathrm{I}}$, and $(D/B)_{\mathrm{I}}$ in Fig. 4 which yields the angular distribution of the differential cross section; and the curve for σ_{I} in Fig. 5 which gives the total cross section in this approximation. The results in Figs. 1 and 2 corresponding to Approximation I show most clearly the effects of including all of the multipoles. At the low energies it may be seen that the magnitude of the final result, the total cross section, is essentially the same as obtains in the simple dipole approximations. As the energy increases the disparity between this and the dipole calculation becomes more pronounced, as indicated for example, by the curves of α and a_s, but the difference is still fairly insignificant at the highest energy we consider. The curves of Fig. 4 representing the angular dependence of the differential cross section show more significant results. There it is observed that even at the lowest energies the forward asymmetry $(C/B)_{\mathrm{I}}$ is appreciable. Thus, it is seen that higher multipoles may have appreciable effects on the angular distribution before they have significant effects on the total cross section. These remarks obtain equally well for Approximation II.

All of the results of Approximation I are independent of any explicit knowledge of the nature of the forces in the deuteron and are dependent upon only the numerical choice of the constants used, i.e., effective ranges, scattering lengths, and binding energy of the deuteron, these values (with the exception of the last) having been obtained from experiments other than photodisintegration. Of these experimental quantities, the triplet effective range, r_{0t} is probably responsible for the largest contribution to the error. As an overall estimate it would seem reasonable to conclude that the numerical results of Figs. 4 and 5 are correct to within 5 percent, this error being due to the uncertainties in the experimental quantities that are used in the numerical calculation. Essentially the same error arises in Approximation II.

B. Approximation II-C

The modifications introduced through Approximation II-C are apparent in Fig. 4 for the effect on the differential cross section, and in Fig. 5 for the effect on the total cross section. The effects of individual terms that are calculated in Approximation II-C are seen in Figs. 1, 2, and 3. The effect of the introduction of the specific potential shape is seen to be most marked for the magnetic spin to final singlet states matrix element M_{ss}'. This result, as indicated before, seems independent of the specific Hulthén form chosen, as evidenced by the good agreement with calculations using a square well. The greatest effect is to decrease the isotropic term as is evidenced by comparison of $(A/B)_{\mathrm{II}}$ to $(A/B)_{\mathrm{I}}$ in Fig. 4. The curve for a' in Fig. 1 shows that the total electric interaction $\mathcal{E}$ matrix element is also decreased by the destructive interference of ${}_0E^1$, though almost negligibly at the lower energies. These

two effects are primarily responsible for the lower total cross section for Approximation II-C as compared to that for the Approximation I. At the lower energies this decrease is due mainly to the smaller total magnetic spin interaction $\mathfrak{M}_{ss}$ matrix element, while at the higher energies the difference is mainly due to the smaller electric interaction matrix element.

The effect of modifying the percentage of exchange force from 50 percent is indicated in Fig. 3 where the dominant term in the matrix element ${}_1E^0$, a_1'', is plotted as a function of energy, and in Fig. 6 where the ratio of the total cross section in Approximation II with 0 percent exchange force, to the total cross section in Approximation II-C with 50 percent exchange force, $\sigma_{II}(0 \text{ percent})/\sigma_{II}(50 \text{ percent})$ is plotted. Both curves indicate the same behavior. Below about 20 Mev the effect of varying the percentage is negligible and therefore difficult to detect experimentally. In fact, the 0 percent cross section is slightly greater than the 50 percent exchange cross section. Above 20 Mev the effects become more pronounced with the 0 percent exchange cross section smaller than the 50 percent exchange cross section, the ratio being 0.87 at 28 Mev. This general result does not seem dependent upon the choice of potential shape[17] since, as mentioned before, the same behavior is obtained with a square well calculation.

Essentially the same arguments apply to the reliability of the numerical results of Approximation II-C as were used for the first Approximation, although the use of the Hulthén wave function diminishes to some degree the error due to the uncertainty in the triplet effective range. We will, however, estimate the error as the same as for the First Approximation.

C. Approximation II-NC

Inasmuch as only approximate wave functions and potentials were used in the noncentral force calculation, the results obtained can only serve to indicate the changes that occur upon the introduction of the tensor force. The most significant modifications to the second Approximation cross section due to the inclusion of a noncentral force are to the angular distribution and may be seen in Fig. 4. Comparing to the terms from Approximation II-C, we see the following changes. First, the isotropic component becomes considerably larger at the higher energies. Thus, the ratio of $(A/B)_{N.C.}$ to $(A/B)_{II}$ is about unity up to around 15 Mev but is nearly two at 28 Mev. Secondly, the forward asymmetry, represented by the two terms $(C/B)_{NC}$ and $(E/B)_{NC}$, is greater at the very low energies, around 6 Mev, but becomes about the same as the central-force case, with the peak slightly shifted, at the higher energies. Finally, the width of the peak in the angular distribution is decreased due to the fact that $(D/B)_{NC}$ is negative in this energy range while it is positive in the central force cases. The total cross section σ_{NC}, Fig. 5, is smaller than σ_{II} at the lowest energies as would be expected due to the lower percentage of S state in the ground state. The fact that the difference between the two cross sections, σ_{NC} and σ_{II}, becomes smaller as the energy increases seems to be a reflection of the relative increase of the isotropic term, both effects apparently being due to the increased importance of transitions from the D state. It is more difficult in this case to see the causes of small changes in the cross sections because of the more complicated spin and angular dependence of the matrix elements and the resultant mixing and interference between terms entering into the calculation of the cross sections.

[17] J. S. Levinger and H. A. Bethe, Phys. Rev. **78**, 115 (1950).

D. Exchange Moment Contribution

The estimated exchange moment contributions to the cross sections are indicated by $(A/B)_{II+XM}$ in Fig. 4 for the effect on the angular distribution, and by the contribution to the second Approximation for central forces total cross section in Fig. 7 where essentially $\sigma_{II+XM}-\sigma_{II}$ is plotted. Since our choice of the strengths for the exchange moments was somewhat arbitrary, these calculations can only serve to indicate the order of magnitude of the effects to be expected. However, these results show that the exchange moment effects may not be inappreciable. Our calculated contribution to the total cross section gives an increase of almost 10 percent of σ_{II} at 28 Mev and the increase of the isotropy in Approximation II-C is nearly fivefold. Unfortunately, because of the other uncertainties of the deuteron problem these effects may not be clearly distinguishable experimentally, if they are present. However, these contributions seem to become more important as the energy increases and it is possible that they may become quite significant at energies above those calculated here.

E. Extension to Higher Energies

The methods used in obtaining our results are expected to be particularly appropriate for similar calculations at higher energies where the higher multipoles would be relatively more important. In fact, Eqs. (10), (18), (22), and (32) could be used in their present form to calculate the corresponding matrix elements, with reasonable accuracy, up to energies of the order of 100 Mev. The Born approximation used for Eq. (16) will, in fact, be better at the high energies. If desired, the calculation could easily be somewhat improved for higher energies by the inclusion of the phase shifts for the D final states, etc.

F. Conclusion

We may conclude, from the results of this paper, that the theoretical estimates for the deuteron photodisintegration, in the energy range here considered, may be

considered to be fairly well bracketed, as is most clearly shown by Fig. 5 for the total cross sections. Certainly, greater accuracy in the experimental quantities used in numerically fixing these cross sections will be almost a prerequisite before refined photodisintegration measurements can distinguish the presence of such effects as are due to tensor forces, exchange forces, exchange currents, or particular well shape. However, as a standard to be used for determining other photo-process cross sections the present calculations indicate that such a calculated result as σ_{II}, as our best approximation to the correct total cross section, can only be considered to be accurate to within 15 percent. About 5 percent of this arises from uncertainties in the values of empirically determined parameters (effective ranges, etc.), while the remainder arises from the uncertainties introduced by lack of knowledge concerning the potential interaction, noncentral interactions, and exchange moments.

ACKNOWLEDGMENTS

The writer gratefully acknowledges his indebtedness to Professor L. L. Foldy for suggesting this problem, and for his invaluable advice throughout the course of the work. The writer is also indebted to Professor M. L. Goldberger for pointing out an error in the original manuscript.

PHYSICAL REVIEW VOLUME 94, NUMBER 6 JUNE 15, 1954

New Neutron-Deficient Isotope of Silver*

B. C. HALDAR† AND EDWIN O. WIIG
Department of Chemistry, University of Rochester, Rochester, New York

(Received February 1, 1954)

Silver-103 of 1.1-hour half-life, produced by bombarding silver with high-energy protons, was identified by following the decay with β-proportional, scintillation, and x-ray proportional counters and by milking the daughter, 17-day Pd^{103}, through seven half-lives. Measurements with a β-ray survey spectrometer showed the presence of conversion electrons of 0.6-Mev energy and positrons of 1.3-Mev maximum energy, both of which decayed with a half-life of 1.1 hours. Aluminum absorption measurements also gave 1.3 Mev as the maximum β^+ energy. Ag^{103} decays in part by K capture.

THE existence of previously unknown Ag^{103} of 1.1-hour half-life was investigated by bombarding silver with protons of energy 80, 100, and 170 Mev in the internal beam of the 130-inch synchrocyclotron of the University of Rochester. Bendel *et al.*[1] have reported bombardment of Pd foil with 12-Mev deuterons and examination of the activity associated with the silver fraction. They observed that conversion lines of 530- and 740-kev associated with the silver activity decayed with half-lives of 1.1 hours, which they could not assign to any known silver isotope. In view of the present results it seems quite likely that they synthesized 1.1-hour Ag^{103} from Pd^{102} by a (d,n) reaction.

EXPERIMENTAL

Silver powder, determined by spectrochemical analysis to contain only traces of copper and possible traces of lead, was wrapped in a 5-mil aluminum foil envelope and bombarded, usually for one hour.

The bombarded sample was dissolved in hot nitric acid containing ions of In, Cd, Pd, Y, Sr, and Rb as carriers. The resulting solution was diluted with water and AgCl precipitated by addition of HCl. The washed solid was dissolved in NH_4OH and the solution scavenged twice with $Fe(OH)_3$. Addition of H_2S to the solution gave a precipitate of Ag_2S, which was washed and dissolved in hot concentrated HNO_3. Dilution and addition of HCl resulted in precipitation of AgCl, which was dissolved in NH_4OH and the $Fe(OH)_3$, Ag_2S, AgCl purification cycle repeated. The final AgCl precipitate was washed with water, alcohol and ether and suitably mounted for counting with β-proportional, scintillation, and x-ray proportional counters. Samples were also prepared for β-ray spectrometer and aluminum absorption measurements.

In milking experiments a known amount of $Pd(NO_3)_2$ as carrier in solution was added to a known weight of purified active AgCl. The mixture was allowed to stand for 45 minutes and then dissolved in NH_4OH solution. At the end of 1.1 hours from the previous precipitation of AgCl, the NH_4OH solution was made acid with HCl and AgCl reprecipitated and separated. The supernatant was scavenged with AgCl, after which palladium dimethylglyoxime was precipitated, separated, and washed. A solution of the precipitate in hot concentrated HNO_3 was again scavenged with AgCl. After dilution of the supernatant, palladium was separated as palladium dimethylglyoxime, washed, dried, mounted, and weighed. The

* This research was supported by a contract with the U. S. Atomic Energy Commission
† Postdoctoral Research Associate in Chemistry.
[1] Bendel, Shore, Brown, and Becker, Phys. Rev. **90**, 888 (1953).